SYTHESIS OF ANTI-ANGIOGENIC DRUG CONJUGATES AGAINST BREAST CANCER

by

Sedef GÜNDAY

B.S., Chemistry, Boğaziçi University, 2011

Submitted to the Institute for Graduate Studies in

Science and Engineering in partial fulfillment of

the requirements for the degree of

Master of Science

Graduate Program in Chemistry

Boğaziçi University

2013

Anneciğime, Babacığıma ve Engin'e

ACKNOWLEDGEMENTS

I would like to express my most sincere gratitude to my thesis supervisor Assoc. Prof. Rana SANYAL for being a great advisor. Her ideas and tremendous support had a major influence on my laboratory work. I appreciate for her endless patience, attention throughout this study.

I wish to express my thanks to Assoc. Prof. Amitav Sanyal for his scientific advice and his helpful discussions regarding all my research in this laboratory.

I wish to express my thanks to Prof. Fethi Şahin for his careful and constructive review of the final manuscript.

I wish to express my great thanks to Ayla Türkekul and Burcu Selen Çağlayan for running NMR measurements supporting my laboratory work.

I would like to extend my deepest pleasure to Özgül Gök, for her care, endless patience and support during my whole research and laboratory work.

I would like to express my thanks to Aslı Erdoğ and Burcu Sümer for conducting biological experiments.

I also would like to thank to all the members of the Chemistry Department of Boğaziçi University and Hülya Metiner.

I also thank my labmates, Özlem İpek Kalaoğlu Altan, Tuğçe Nihal Gevrek, Betül Bingöl, Nergiz, Sadık, Filiz, Merve, Duygu, Fatma, Yasemin, Derya, Rabia, Özge and my hoodmate Mehmet Arslan and my former labmates Nazlı Böke, Merve Coşar, Melike Eceoğlu, Pelin Ertürk, Merve Türksoy for their friendship and endless support and for their companionship.

Finally, my deepest thanks go to my whole family and Engin for their endless love, support and encouragement throughout these years.

ABSTRACT

SYTHESIS OF ANTI-ANGIOGENIC DRUG CONJUGATES AGAINST BREAST CANCER

Angiogenesis, formation of new blood vessel, has a primary role in local growth and distant metastasis in breast cancer. By an anti-angiogenic therapy for breast cancer, this process can be inhibited. Different from conventional chemotherapy agents, selectivity of anti-angiogenic agents toward newly formed and disorganized blood vessels around the tumor is an attractive tool for reduced toxicity. Polymer-drug conjugates are designed to achieve improved drug targeting to the tumor, to reduce drug toxicity and to overcome the mechanisms of drug resistance. By conjugation of a therapeutic agent to a water soluble polymer, its aqueous solubility can be significantly improved. Therapeutically effective concentration of an agent can be achieved when a particular drug delivery profile like rate and duration are designed. Moreover, accumulation of these macromolecules only in the tumor tissue can be accomplished by "enhanced permeability and retention effect". In this thesis, we disclose the synthesis of novel poly(ethylene glycol) methacrylate based copolymers containing drug units as side chains by free radical polymerization, analytical characterization and examination the effect of the prepared conjugates on human umbilical vein endothelial cells (HUVECs) *in vitro*.

ÖZET

MEME KANSERİNE KARŞI ANTİ-ANJİYOJENİK İLAÇ KONJUGATLARININ SENTEZLENMESİ

Yeni kan damarı oluşumu olan anjiyojenezin, meme kanserinde hem lokal tümör büyümesinde hem de metastazda birincil rolü vardır. Anti-anjiyojenez tedavisiyle her iki süreçte de hastanın yararına etkide bulunulabilir. Klasik kemoterapi ajanlarından farklı olarak anti-anjiyojenez ajanlarının yeni oluşan ve organize olmayan tümör etrafındaki kan damarlarına karşı seçiciliği toksisitenin azaltılması için ilgi çekici bir araçtır. Polimer-ilaç konjugatları tümör hedeflemek,, ilaç toksisitesini azaltmak veya ilaç direnç mekanizmalarını aşmak için tasarlanabilir. Bir ilacın sudaki çözünürlüğü, suda çözünebilen bir polimer konjugasyonuyla önemli ölçüde geliştirilebilir. İlacın vücutta dağılım hızı ve süresi istenilen teröpatik olarak etkili konsantrasyonu elde etmek için özel olarak tasarlanabilir. Dahası bu makromoleküllerin sadece tümörlü dokularda birikimi "gelişmiş geçirgenlik ve alıkonma etkisi" metodu ile sağlanabilir. Bu tezde, serbest radikal polimerizasyon yöntemiyle sentezlenmiş yan zincirleri ilaç etken maddesi içeren polietilen glikol metakrilat bazlı yeni kopolimerlerin hazırlanması, analitik karakterizasyonu ve hazırlanan konjugatların *in vitro* olarak insan umbilikal ven endotel hücreleri (HUVEC) üzerine olan etkisinin incelenmesi açıklanmaktadır.

TABLE OF CONTENT

LIST OF FIGURES

LIST OF TABLES

LIST OF SYMBOLS

J	Coupling constant
υ	Frequency

LIST OF ACRONYMS/ABBREVIATIONS

AIBN	Azobisisobutyronitrile
CA4	Combretastatin A4
CA4P	Combretastatin A4 phosphate
$CDCl_3$	Deuterated chloroform
CH_2Cl_2	Dichloromethane
DCC	Dicyclohexanecarbodiimide
DIEA	Diisopropylethyl amine
DIPC	N,N'-Diisopropylcarbodiimide
DMAP	N,N'-Dimethylaminopyridine
DMF	Dimethylformamide
DOX	Doxorubucin
EtOAc	Ethyl Acetate
FT-IR	Fourier Transform Infrared
GPC	Gel Permeation Chromotography
HPLC	High Performance Liquid Chromatography
HUVEC	Human Umbilical Vein Endothelial Cell
Hz	Hertz
LC-MS	Liquid Chromatography-Mass Spectrometry
MeOH	Methanol
MAC	Methacryloyl chloride

NMR	Nuclear Magnetic Resonance
PT	Polymer Therapeutics
PEG	Poly(ethylene glycol)
PEGMA	Poly(ethylene glycol) monomethyl ether methacrylate
PPX	Poly-L-glutamic acid-paxlitaxel conjugate
TEA	Triethylamine

1. INTRODUCTION

1.1. Cancer

Cancer characterized by uncontrolled cell division and reduced cell death, is essentially a genetic disease due to DNA damage at the molecular level. Since the cells cannot control themselves called apoptosis, fast grow in the cancer cells, tissue infiltration, reduced cell death, supplement of blood to the tumor due to newly formed vessels inside the tumor, metastasis to surrounding organs in the body, and dysfunction of affected organs are occurred [1]. In the blood supplement process to the tumor and metastasis, angiogenesis plays a crucial role.

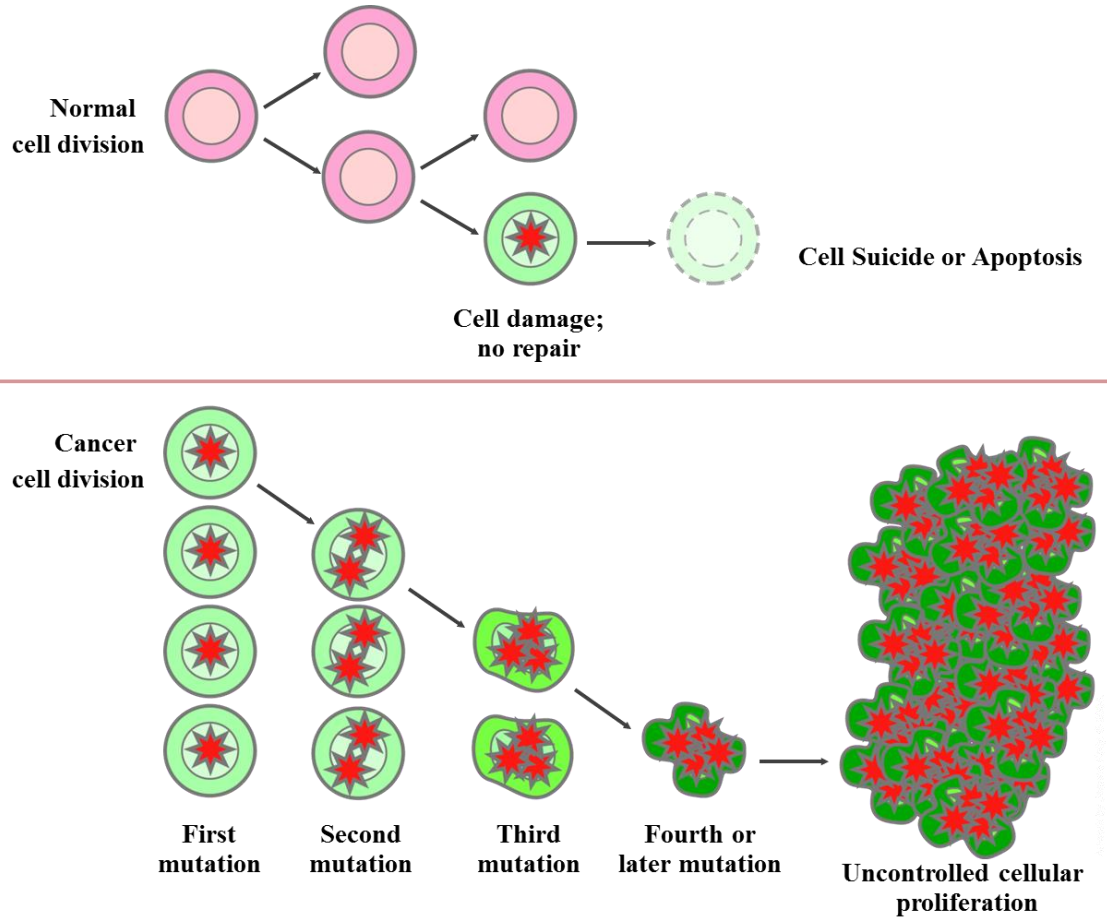

Figure 1.1. Normal cell versus cancer cell divisions [2].

1.2. Chemotherapy

In order to prevent the abnormal division and growth of tumor cells, chemotherapy is a very common way to treat cancer by delivering anticancer agent to tumor. Anti-cancer drugs which are small molecules, affect quickly dividing cells nonspecifically in both tumor tissue and healthy tissue with high growth profile. As a consequence, selectivity of the agents becomes poor. Besides, toxicity is dose limiting in this system since side effects are observed such as bone marrow toxicity (decrease in white blood cells (WBC) and red blood cells (RBC), hair loss, cardiotoxicity, nausea, gastrointestinal and skin problems and vulnerability to illness. That is why the amount of drugs given to patient is limited. Moreover, genomic instability of tumor cells leads to drug-resistance which decreases the activity of chemotherapy drugs further [3, 4].

1.3. Angiogenesis

Angiogenesis appears when the newly formed blood vessels grow into a wound space followed by injury. Healing of any skin wound can occur through angiogenesis. Damaged vasculature is needed to be repaired. Besides, supply of nutrients in high amount from bloodstream is also required in the prolonged cell activity for local healing [5].

Angiogenesis in cancer is very similar to wound angiogenesis described above. However, unregulated angiogenesis is essential to tumor growth and metastasis which affect cell growth negatively.

Non-angiogenic solid tumors are dramatically influenced by their microenvironment to supply oxygen and nutrients which can reach inside of the tumors (1-2 mm^3) by simple diffusion. However, cellular hypoxia (oxygen deficiency in the cells) begins when the solid tumor reaches 2 mm^3. Then the angiogenesis process is initiated with the release of pro-angiogenic factors such as vascular endothelial growth factor (VEGF), tumor necrosis factor-α (TNF-α) by the tumor cells to the surrounding normal cells so that certain genes in the normal cells are activated and new blood vessels start to grow. (Figure 1.2) When the new blood vessels create a network (neovascularization), cancer cells can disseminate to the other tissues, leading to metastasis [6, 7].

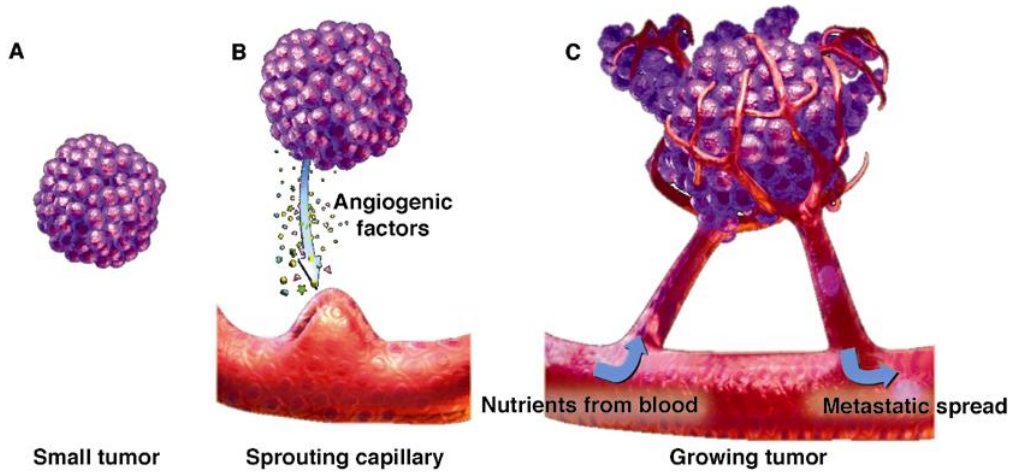

Figure 1.2. General scheme of the angiogenic switch [2].

1.4. Angiogenesis Inhibitors

Tumor induced process angiogenesis involves lots of growth factors and their receptors, cytokinase, proteases and adhesion molecules which may bring about uncontrolled growth of endothelial cells, migration of endothelial cells, or proteolytic degradation of the extracellular matrix, resulting in the formation of a functional vessel with a lumen. Consequently, for anti-angiogenic therapy it is given targeting opportunities and various targets are exhibited for the treatment [8, 9].

Angiogenesis inhibitors disrupt the events mentioned in previous paragraph resulting in prevention of new blood vessel formation or damage existing vessels. In other words, they disclose specific targeting to the endothelial cells directly in contact with blood circulation, not to cell cycle as usual chemotherapy. Hence, they are relatively less toxic than usual chemotherapy agents and exhibit lower risk of drug resistance [6, 10].

On the other hand, the drawback of many anti-angiogenic agents is to have small size and therefore poor pharmacokinetic and biodistribution profile. As a result, relatively small amounts of the agents reach the targeted site causing low efficacy [6].

Today there are many angiogenesis inhibitors that are in clinical trials or in the market. For example, Erlotinib (Tarceva®, Genentech) and gefi-tinib (IressaTM,

AstraZeneca) are reversible tyrosine kinase inhibitors that target the epidermal growth factor receptor (EGFR). Another targeted agent, bevacizumab (Avastin®, Genentech), a monoclonal antibody that binds vascular endothelial growth factor (VEGF) is in phase III clinical trial. Besides, Sorafenib, Sunitinib, Imatinib, Pazopanib as tyrosine kinase inhibitors are in cilinical trial [11, 12].

1.4.1. Combretastatin A4

For the treatment of cancer many anti-microtubule agents such as Taxol and Vinca alkaloids have been used for a long time. Yet, among the tubulin binding agents as (i) microtubule stabilizing agents, (ii) vinca site binding agents, and (iii) colchicine site binding agents, the last one is not used as a commercial drug in clinic for cancer. Many natural compounds and synthetic small molecules are consisted of this class [13].

Through all the colchicine site agents, combretastatin A4 (CA4, Figure 1.3) which is a natural cis-stilbene product isolated form the bark of African willow tree Combretum caff rumin 1982, has a remarkable interest in the last decade or so. CA4 has a significant cytotoxicity and inhibitory activity on tubulin polymerization which is exhibited by the mechanism of binding to the colchicine site (ring A in Figure 1.3). Moreover, CA4 is one of the few tubulin binding agents which was proved to have selectivity on vascular targeting activity, and to destroy tumor blood vessels particularly. As a consequence, tumor cell death is occurred. The importance of 3,4,5-trimethoxy substitution on the A-ring (Figure 1.3) and the cis-orientation between the two aryl rings were displayed by the work of Hsieh and Nam for efficient binding to tubulin [12, 14].

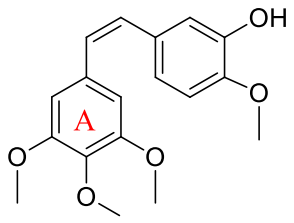

Figure 1.3. Combretastatin A4.

As reported in the literature [9], CA4 seems to interfere with the organization of the cytoskeleton. In Figure 1.4 proliferating HUVECs were (a) untreated, or (b) treated with combretastatin A4 (3 mol/L) for 6 h and stained with a monoclonal antibody against β-tubulin conjugated to cyanine 3 (red) and visualized by confocal microscopy. It is displayed that microtubule organization in HUVECs is influenced by CA4 exposure. So the cytoskeletal network in Figure 1.4 is the proof of its noticeable disruption leading to rounding-up of HUVECs and their separation from the substratum.

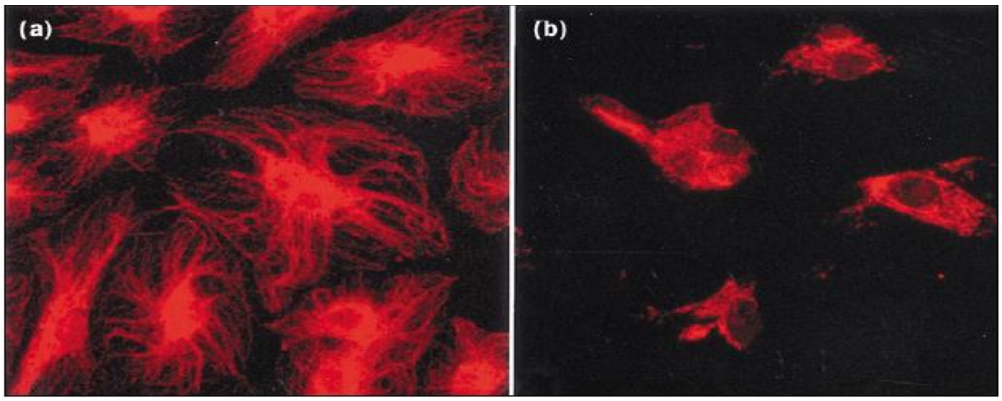

Figure 1.4. Cytoskeletal disruption induced by CA4 [9].

Even though CA4 has very strong tubulin binding capacity, it has poor water solubility and consequently short half-life. Hence, its hydrophilic prodrug, CA4 phosphate (CA4P, Figure 1.5) has being investigated. On the other hand CA4P still has cytotoxicity problems. Since it is small molecule it can easily penetrate into all kinds of cells. To make CA4 more effective there are promising biological systems being studied for decades.

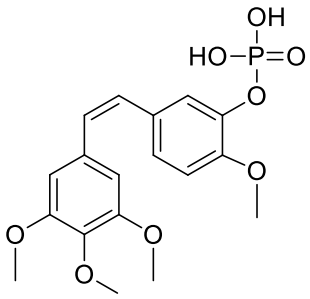

Figure 1.5. Combretastatin A4 Phosphate.

1.5. Polymer Therapeutics

Many therapeutic agents administered systemically have low-molecular weight. Hence they display poor pharmacokinetics profile in which non-specific bio-distribution, short half-life and quick systemic elimination are observed. As a result, relatively small amounts of the drug reach the desired site, and critical side effects as well as low efficacy are observed in the therapy. To be able to avoid or improve those drawbacks, macromolecules as carriers have being improved over 50 years. Then it was proposed by Helmut Ringsdorf in 1975 the analysis of a polymer bounded to a drug, which indicated an excellent complete biologically active delivery system [15].

The Ringsdorf model (Figure 1.6) firstly contain a biocompatible polymer backbone bound to following components: (i) a solubilizer, which contributes to hydrophilicity to provide water solubility to whole macromolecule; (ii) a drug, usually attached to the backbone via a linker; and (iii) a targeting moiety performing to bind the carrier to the biological targeted site[16].

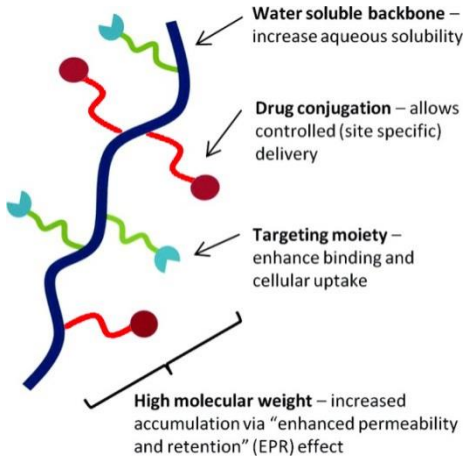

Figure 1.6. The Ringsdorf polymer-drug conjugate model for drug delivery [16].

Polymer therapeutics (PT, Figure 1.7) have been defined as models in which drugs are conjugated to biocompatible polymers as well as other polymeric carrier systems. These systems primarily contain polymer–protein conjugates, drug–polymer conjugates, and in recent years supramolecular drug-delivery systems as well as other well-defined nano-sized systems [17]. As mentioned before Ringsdorf had suggested a perfect mechanism which later opened a gate to PT whose pioneer by R. Duncan and her coworkers.

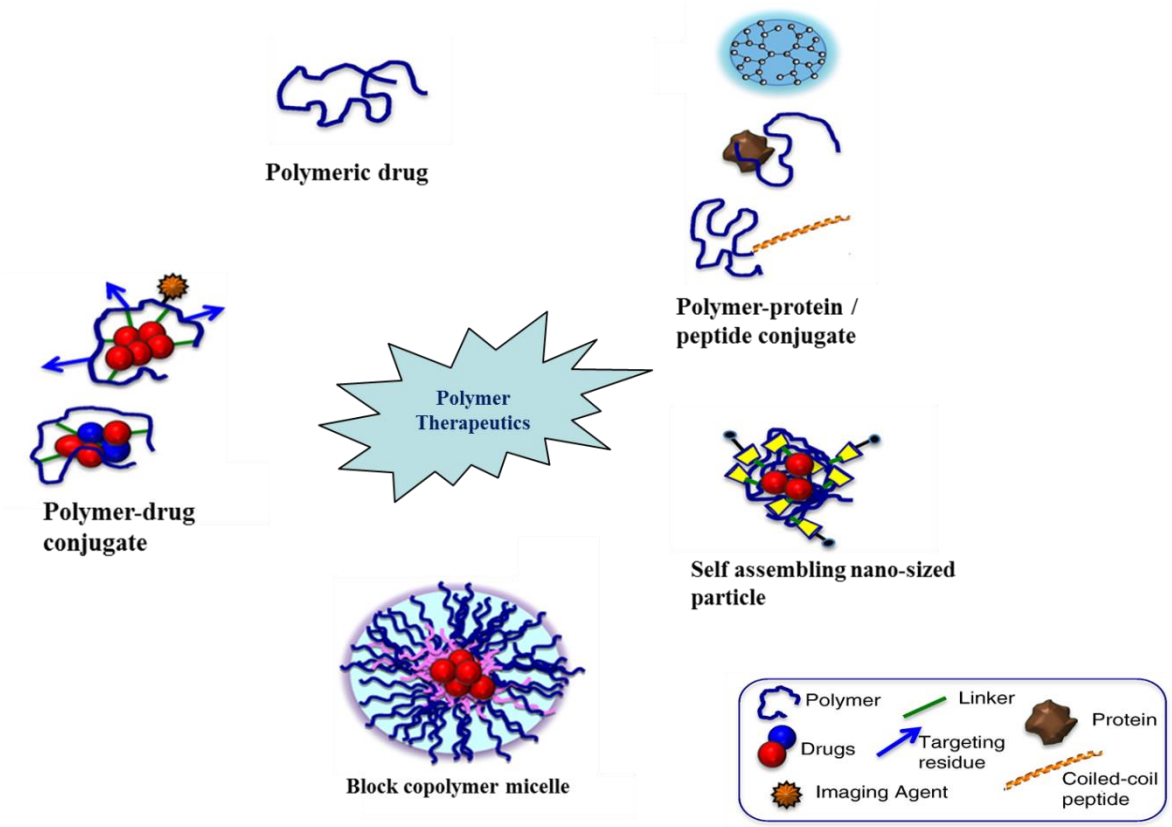

Figure 1.7. Schematic representation of subclasses of Polymer Therapeutics [18].

The molecular carriers chosen for polymer therapeutics should be first water soluble so that solubility of small drug molecules, which exhibit poor bioavailability due to low water solubility, (i.e. CA4) can dramatically be improved through conjugation to the carriers. Next, they should be biodegradable and/or being able to eliminate from the organism so that toxicity of the carriers can be avoided. Besides, the drug conjugated directly or via a linker onto the polymer backbone should release over a defined time interval at target site providing controllable drug delivery. By that way, drug delivery profile with rate and duration can be improved to create the planned therapeutically effective concentration and to avoid the maximum tolerated dose causing side effects and toxicity [15, 16]. Moreover, polymer therapeutics are very useful to improve pharmacokinetics and biodistribution of the drugs exhibited a short plasma circulation time resulting from rapid metabolism, clearance or for drugs exhibited off target toxicities (i.e., anticancer agents). There is also one important advantage of the macromolecules which is the incorporation of targeting units performing to carry the drug to the pharmacologically active site [16].

To have a great pharmacokinetics and pharmacodynamics profile of the therapeutic drug the choice of backbone for the polymeric carriers is very effective. The properties of a polymer such as molecular weight, polydispersity, charge, architecture, and hydrophilicity, determine the stability and solubility of the conjugated drug, loaded amount of the drug, its biodistribution, excretion through the kidneys and its interaction with the immune system. In a conjugate, the backbone of polymeric unit can be biodegradable, semi-biodegradable and also non-biodegradable but should be removable [15].

Today, there are various polymer drug conjugates as accepted therapeutic agents in clinical trials. In Figure 1.8 examples of the conjugates with HPMA backbone are exhibited. [19]. In order to reduce cytotoxic effects of the drugs (DOX in a and b, and Taxol in c), they are conjugated to water soluble synthetic HPMA polymer through GFLG linker in the first 2 conjugates and ester linker in c.

In HPMA-DOX conjugates (PK1 and PK2, Figure 1.8), the tetra-peptide linker provide selectively drug release in the tumors by the help the functionality in the lysosomal enzymes. The conjugates demonstrates prolonged blood circulation in vivo, and enhanced tumor-to-blood ratio as a function of time, and improved C_{max} in tumors after intravenous administration [20].

Another conjugate is taxol, one of the most clinically active cytotoxic agents, bounded poly-L-glutamic acid (PPX) (c, Figure 1.8). It was created to improve the efficacy and safety of taxol through conjugation to the biodegradable poly-L-glutamic acid via ester linker. PPX indicates prolonged plasma circulation which was achieved by accumulation of the carrier in the tumor vasculature at higher concentrations [21].

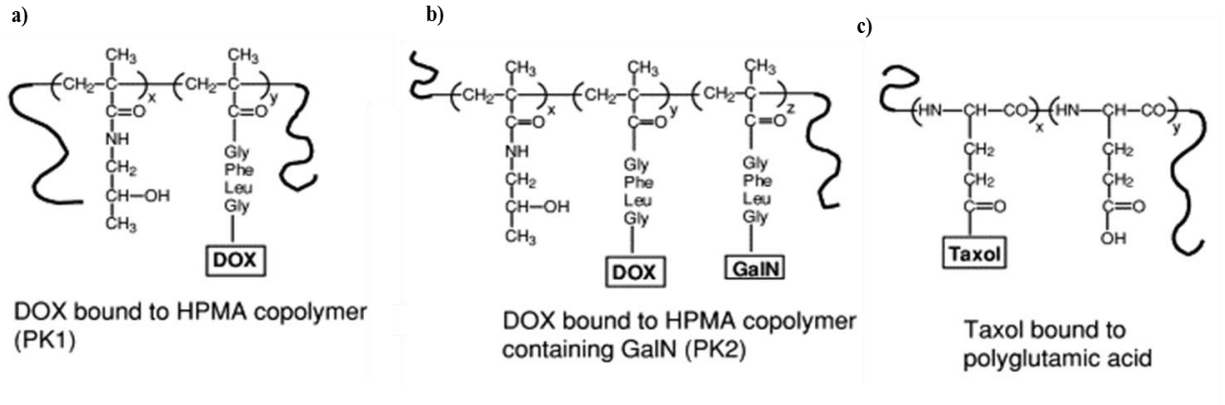

Figure 1.8. Examples of P-D conjugates with HPMA backbone in clinical trials [19].

Some of the PEG based therapeutics such as PEG-SN38 (EZN-2208, Figure 1.9a), PEG-Camptothecin (Pegamotecan, Figure 1.9b) are also in clinical trials. PEG has just two reactive groups in one chain which is the main drawback of PEG as drug carrier, causing essentially low drug loading. To enhance its low loading capacity, a dendron structure at the PEG's end chain has been suggested. Enzon has recently developed a conjugate named SN38, an active metabolite of camptothecin (CPT), with four armed PEG. Pegamotecan (Figure 1.9b) developed by Enzon Pharmaceuticals, Inc. consists of two CPT molecules conjugated to difunctional PEG using an alaninate ester linkage. Free CPT must be released from the PEG to show pharmacological action. In Pegamotecan, the active hydroxyl unit of CPT hindered by the alaninate linker can stabilize the CPT molecule into its active lactone conformation.

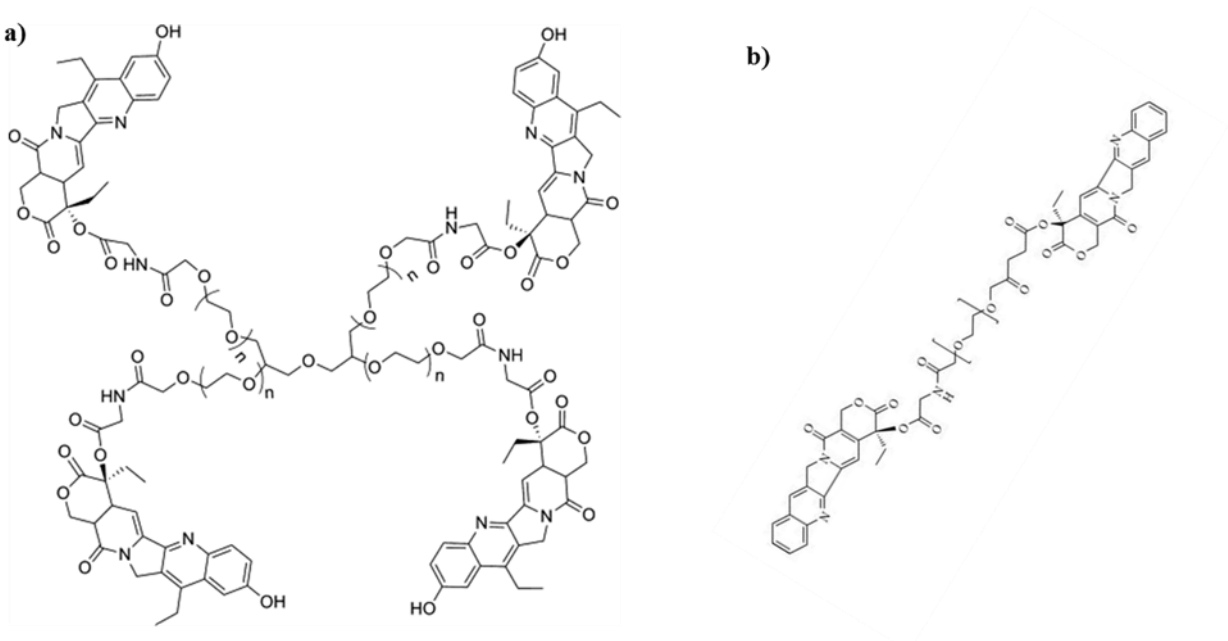

Figure 1.9. Examples of PEG based therapeutics in clinical trials [22].

The principle for using polymeric macromolecules as carriers to deliver angiogenic inhibitors and other therapeutic agents is based on the biological idea explained by Matsumura and Maeda in 1986, known as EPR (Enhanced Permeability and Retention) effect (Figure 1.10). It was suggested that uptake of macromolecules by solid tumors can be enhanced because pathophysiological characteristics of solid tumors are different from healty tissues, such as broad angiogenesis and hence vascular abnormalities (such as leaky and twisted blood vessels), and damaged lymphatic drainage. When the macromolecules

penetrate the interstitium, they get preserved there by lymphatic drainage defficiency in tumor tissue and accumulate at high concentrations [15].

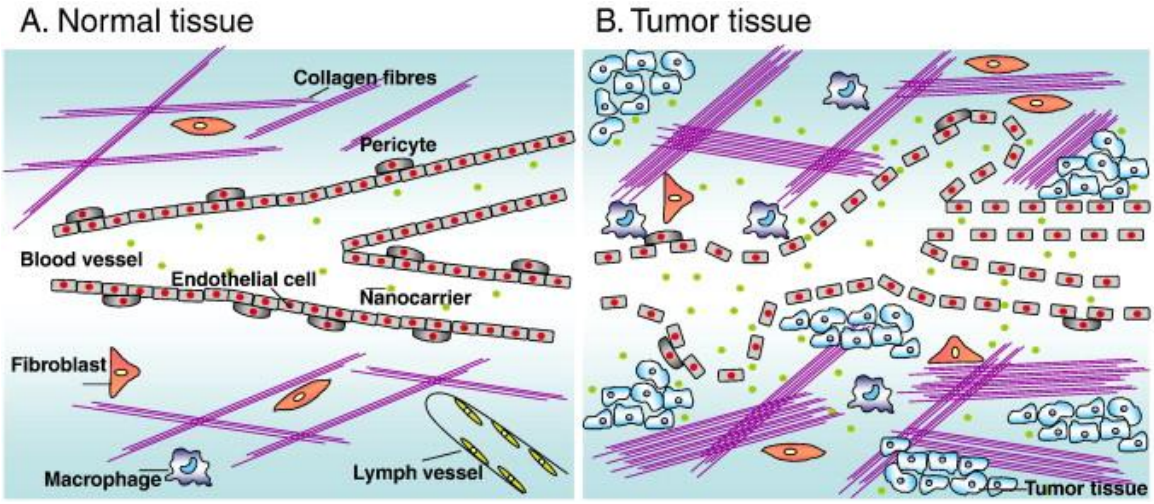

Figure 1.10. Normal and tumor tissues are physiologically different from each other due to EPR effect which explains the passive targeting of nanocarriers [6].

Compounds with low molecular weights show rapid and non-specific drug delivery into both healthy and normal tissues through endothelial cell layers of blood capillaries whereas macromolecules like therapeutic agents have specific and slow diffusion. Hence, commercial agents cause undesired side effects and due to small size fast renal clearance is appeared. To create a polymeric carrier for drug delivery the size of the macromolecule is a crucial parameter because it will influence the pharmacokinetic profile and the amount of the drug accumulated at the targeted site. The normal renal threshold is in the range of 30–50 kDa. Therefore, to achieve an optimum balance in between these ranges, the molecular weight of the polymeric backbone should be preferred in the range of 20 to 200 kDa for proper drug delivery system [8].

When the macromolecules entered the tumor tissue due to EPR effect and they accumulate there at high concentration, degradation of the conjugates and/or cleavage of linkers occur due to thermal, pH or enzymatic difference in tumor tissues (Figure 1.11).

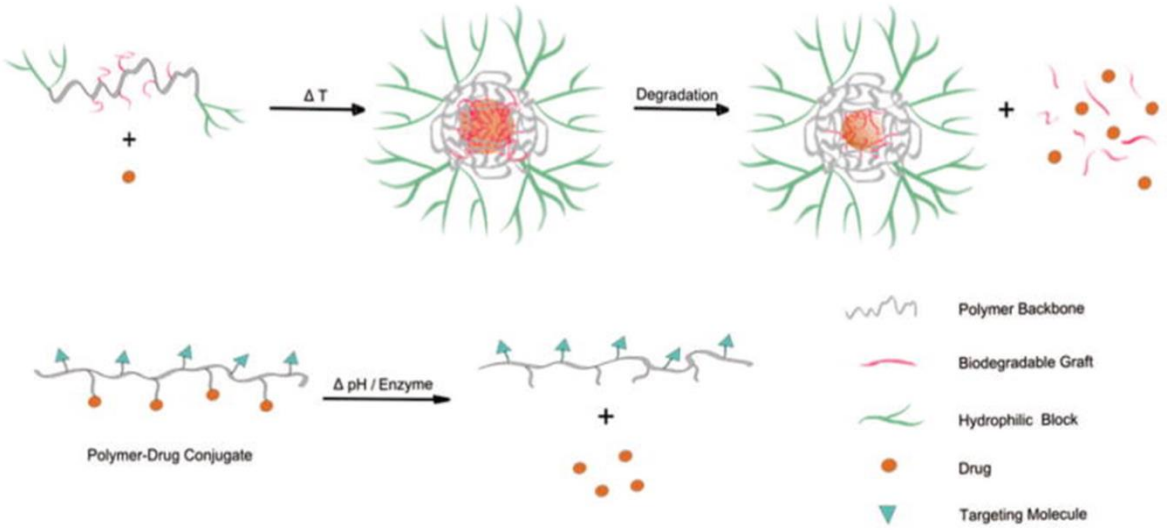

Figure 1.11. Illustration of temperature, pH/enzyme sensitive drug delivery systems [23].

As mentioned before, polymer based therapeutics offer release profile in a control manner. This can be proved by an anti-angiogenic agent TNP-470 bounded to HPMA copolymer (Caplostatin, Figure 1.12a). In the presence of lysosomal enzyme Cathepsin B which provides enzymatic cleavage to GFLG linker, TNP-470 release from the conjugate much more effectively (Figure 1.12b).

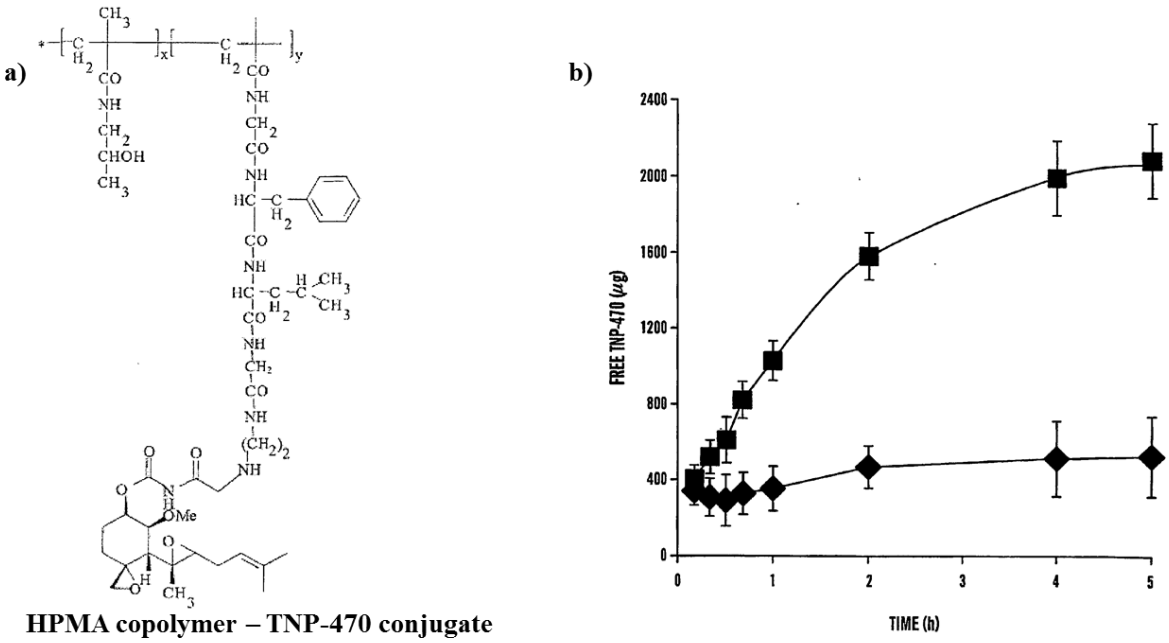

Figure 1.12. (a) Structure of HPMA copolymer–GFLG-ethylenediamine–TNP-470. (b) in vitro release of TNP-470 from HPMA copolymer in the presence (■) or absence (♦) of cathepsin B [24].

By taking all the advantages of polymer therapeutics, novel polymer drug conjugates can be synthesized to enhance the pharmacokinetics profile of angiogenic inhibitor CA4. A conjugate with water soluble side chain and a small drug attached to backbone which has high enough molecular weight can be constructed. In this way, accumulation in the targeted site due to EPR effect, controllable release profile in cancer cells and more effective therapeutics will be provided.

2. AIM OF THE STUDY

The aim of our study is to synthesize and covalently attach combretastatin A4 (CA4) molecule to water soluble and biocompatible polymer, followed by *in vitro* evaluation of this construct. Although CA4 is a very potent vascular disrupting agent, its limited water solubility hinders its potential use in the clinic. Therefore, a water soluble construct could potentially provide benefit. The planned construct will not only bring solubility, but also by carrying a number of kargo molecules on the same molecule, will increase the local concentration of the delivered drug molecule. The polymer of choice is the highly water soluble PEG based acrylate, where the number of drug molecules can be tailored as needed. The large molecular weight of the polymer will help accumulate in tumor passively, utilizing EPR effect.

Following the preparation of the above mentioned construct, it will be tested as an anti-angiogenic agent against human umbilical vein endothelial cells (HUVECs) *in vitro* and release profiles will be investigated under different conditions.

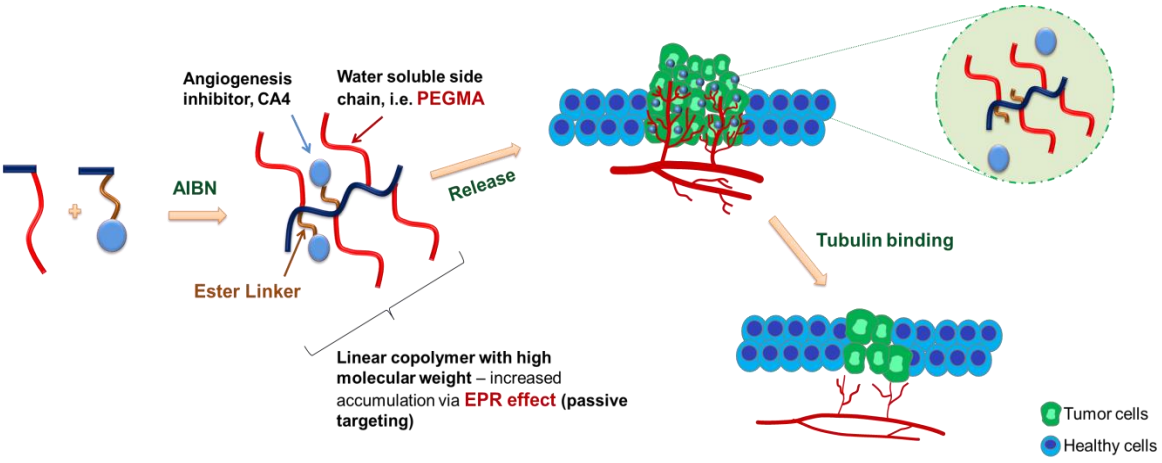

Figure 2.1. General scheme of aim of the study.

3. RESULTS AND DISCUSSION

3.1. Sythesis of Drug Conjugates via Free Radical Polymerization

In this study, novel poly(ethylene glycol) methacrylate based linear copolymers bearing water insoluble drug units as side chains were synthesized by free radical polymerization. Vascular disrupting agent CA4 was synthesized and then copolymerized to obtain water soluble construct.

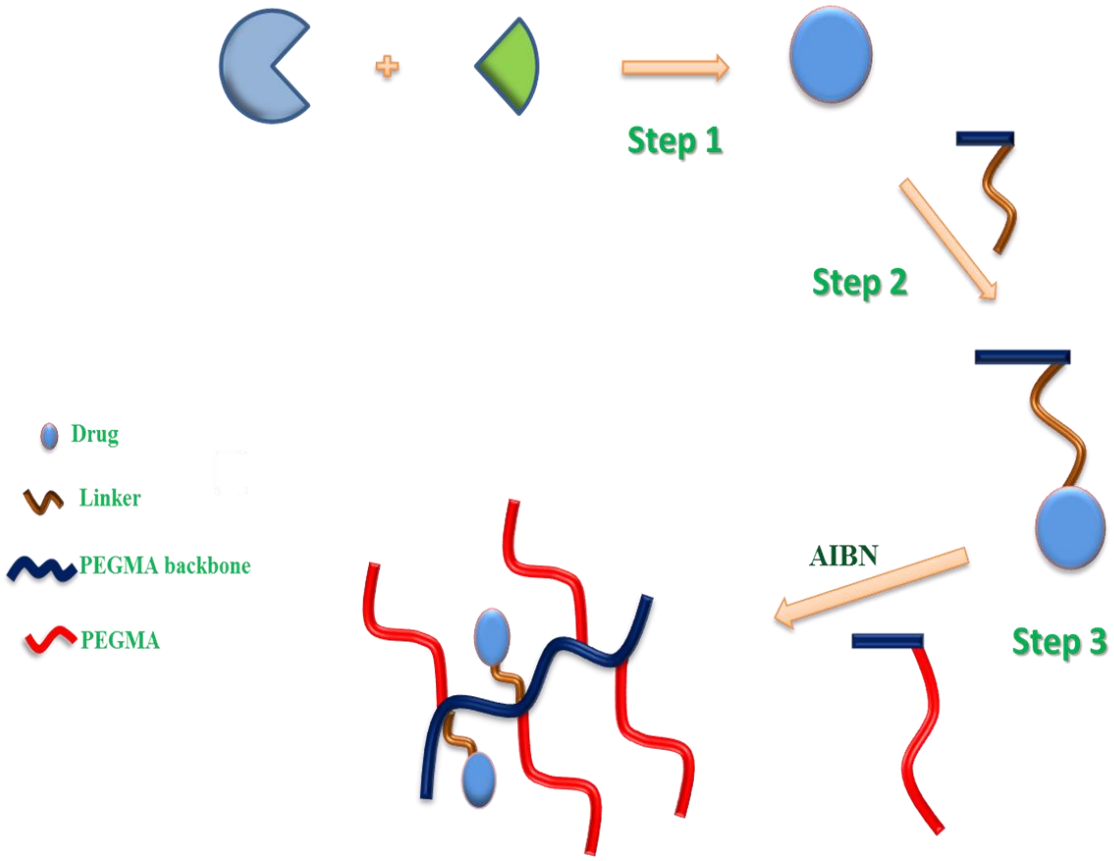

Figure 3.1. General scheme of polymer-drug conjugate synthesis.

As shown in Figure 3.1, the first step is to synthesize drug molecule CA4 which was followed by preparation of the monomer. Subsequently, drug monomer and PEGMA were copolymerized to form linear random copolymers in the presence of AIBN as initiator.

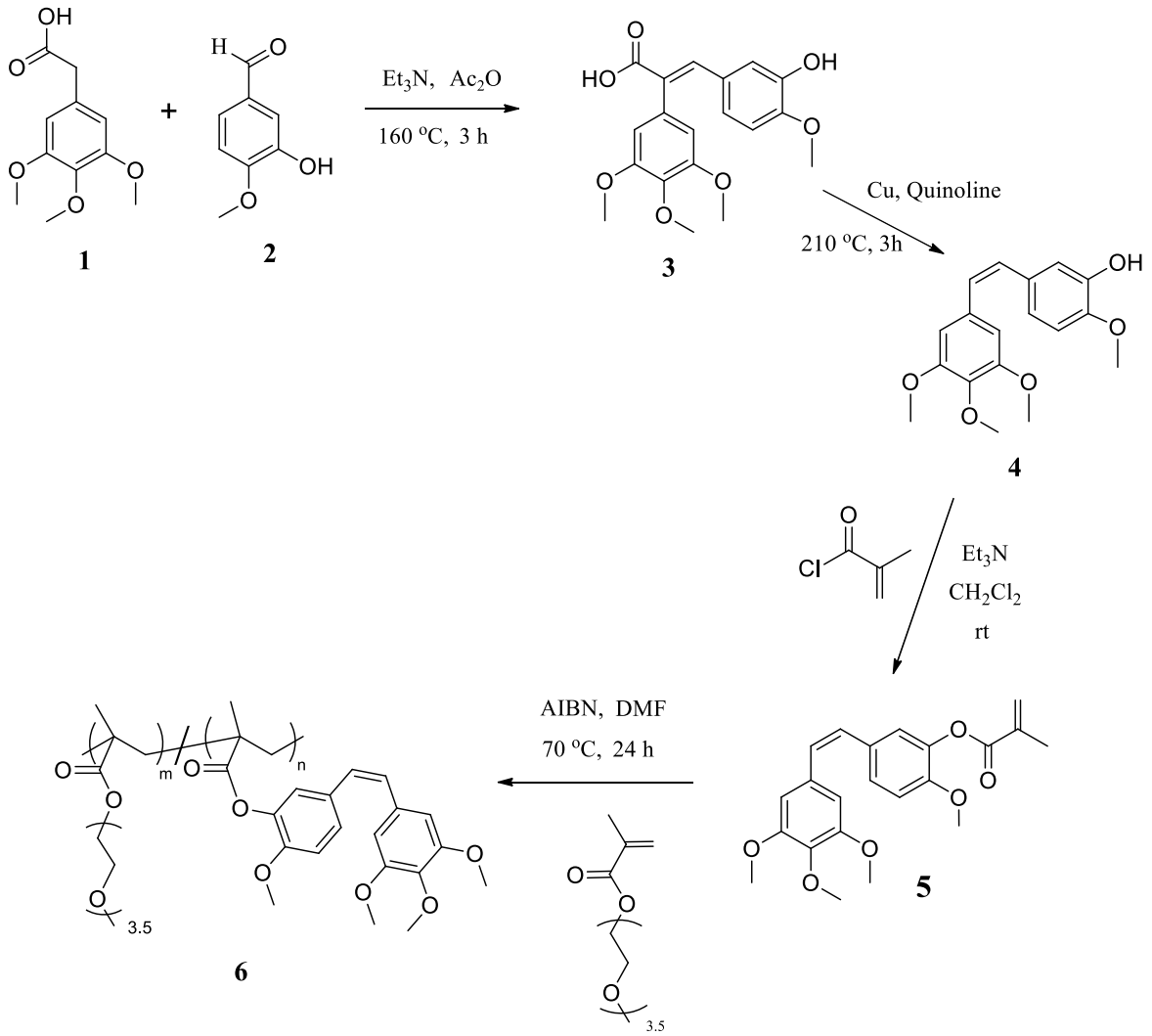

Figure 3.2. Chemical representation of synthesis of p-d conjugates with ester linker.

Combretastatin A4 was synthesized according to literature procedure (Figure 3.3) [25]. Propenonic acid **3** was obtained by Perkin condensation of 3-hydroxy-4-methoxybenzaldehyde (**2**) and 3, 4, 5-trimethoxyphenylacetic acid (**1**) in the presence of acetic anhydride and triethylamine. Subsequently, CA4 (**4**) was synthesized via decarboxylation of propenoic acid **3** with copper in quinolone at 210 ^{o}C.

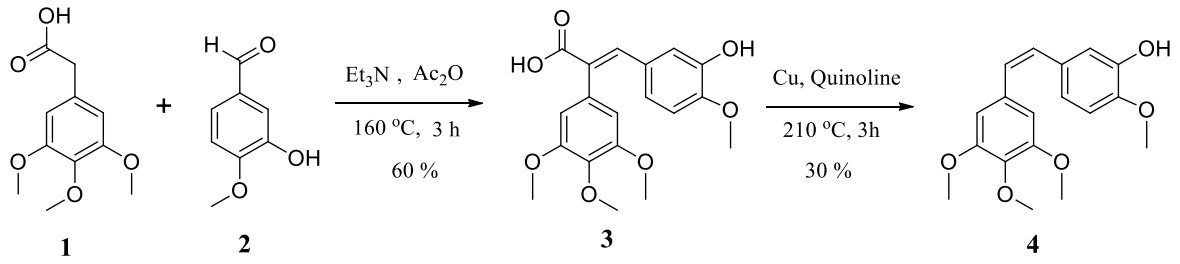

Figure 3.3. Synthesis of Combretastatin A4 (**4**).

Cis isomer of CA4 is more effective than the trans one. Hence, it was wanted to have cis isomer rather than trans isomer of CA4. For that purpose, the crude product could be purified by recrystallization to remove the trans isomer. However, its purification was performed by column chromatography since the amount of crude was not enough to be able obtain all cis isomer. Then it could be proved by ^{1}H NMR (Figure 3.4) if trans isomer was removed.

The compounds **3** and **4** were also characterized and compared via FT-IR (Figure 3.5).

According to ^{1}H NMR assignment of CA4 (Figure 3.4) hydroxy proton is observed at 5.50 ppm as singlet. Alkenic protons at 6.42 ppm are seen as doublet. Protons of methoxy group are seen as singlets. According to the literature [25] ^{1}H NMR characterization for trans isomer of CA4 indicated the peak at 7.24 ppm (1H, t, J=2.5, Figure 3.4) belongs to the proton f in trans isomer. Besides, hydroxyl proton at 5.50 ppm (Figure 3.4) is not a singlet since the proton in trans isomer of CA4 has another singlet different than in cis isomer [25]. These results prove that trans isomer of CA4 was also produced.

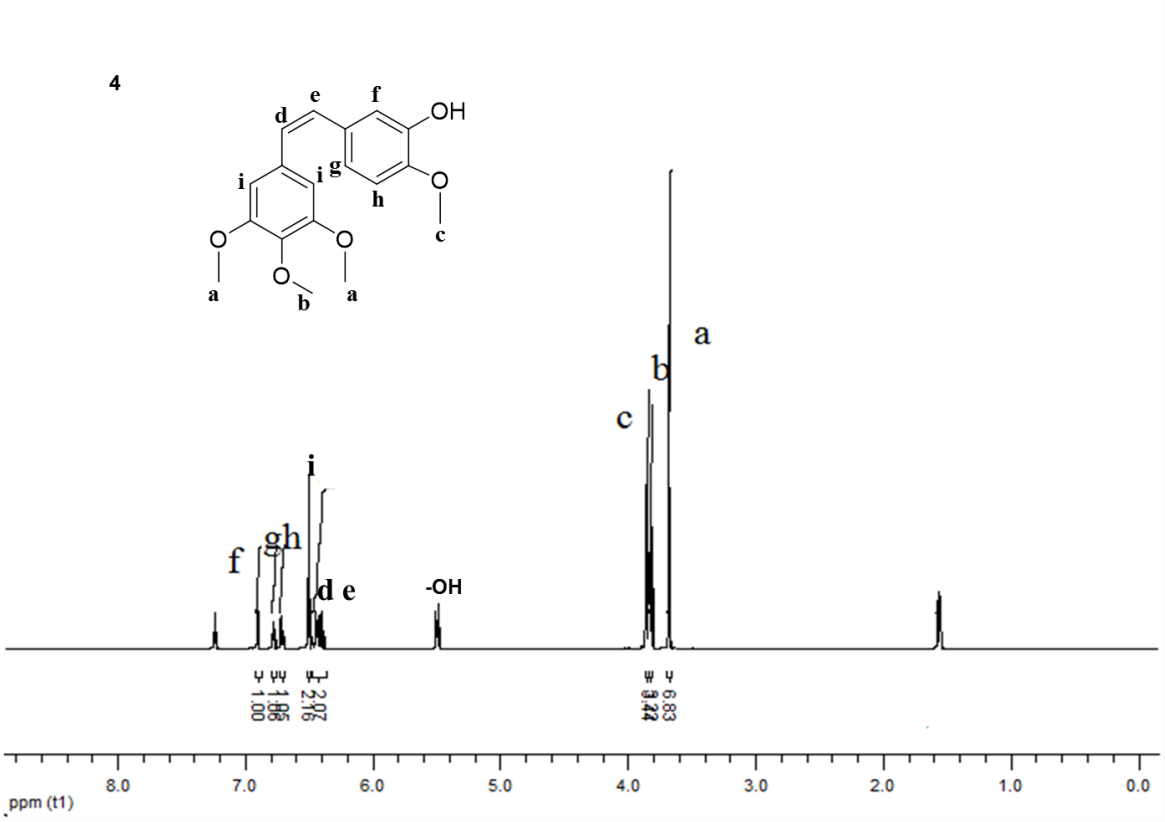

Figure 3.4. ^{1}H NMR Spectrum of CA4 (**4**).

According to FT-IR Spectrum comparison of **4** to **3** (Figure 3.5) carbonyl stretching of propenonic acid at 1662.8 cm^{-1} disappeared after decarboxylation to form CA4 (4). C-C double bond stretching between two aromatic rings of propenoic acid gives an observable peak at 1583 cm^{-1}. It shifted to 1577 cm^{-1} in CA4 (**4**) after decarboxylation of the carboxylic acid group. Besides, sharp C-O stretching is observed in spectra of both propenonic acid (**3**, 1501 cm^{-1}) and CA4 (**4**, 1504 cm^{-1}).

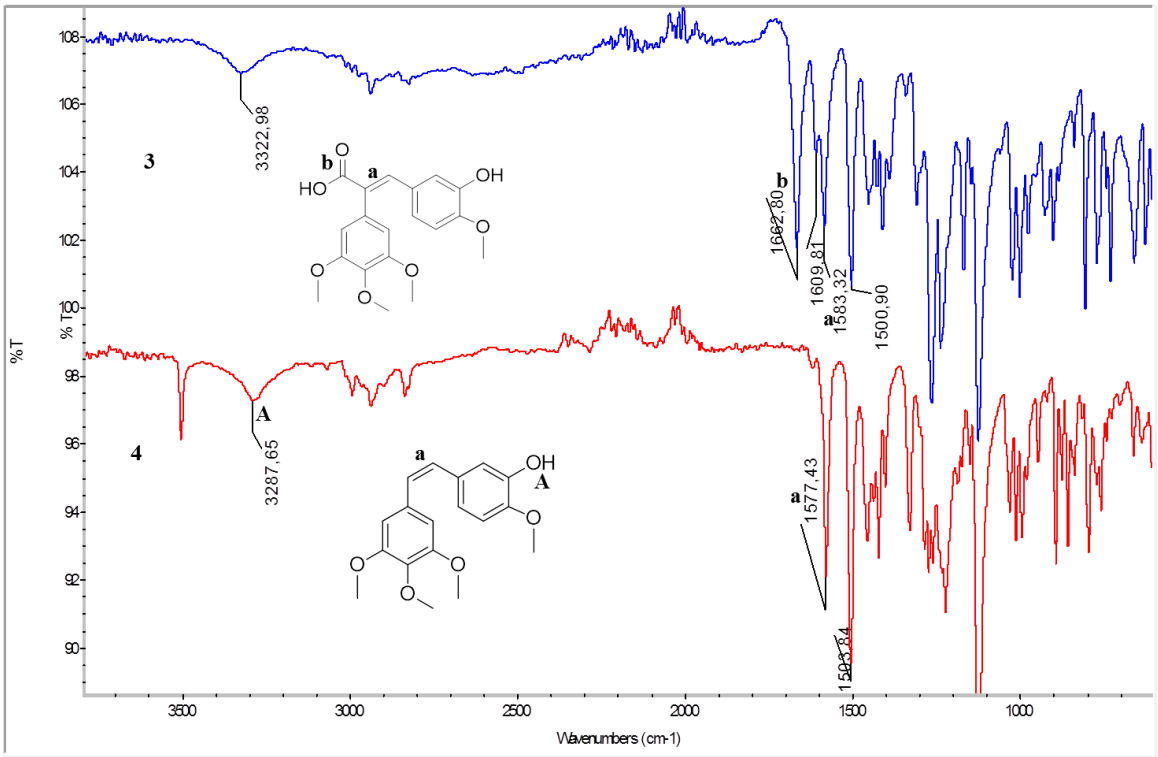

Figure 3.5. Comparison of FT-IR spectrum of compound **3** and **4**.

To synthesize the drug bearing monomer **5**, CA4 was reacted with methacrylolyl chloride in the presence of TEA in dichloromethane (Figure 3.6). The formation of ester bond is essential because it is hydrolyzable in the body. Hence, its hydrolysis would yield free CA4 upon release from the final polymer.

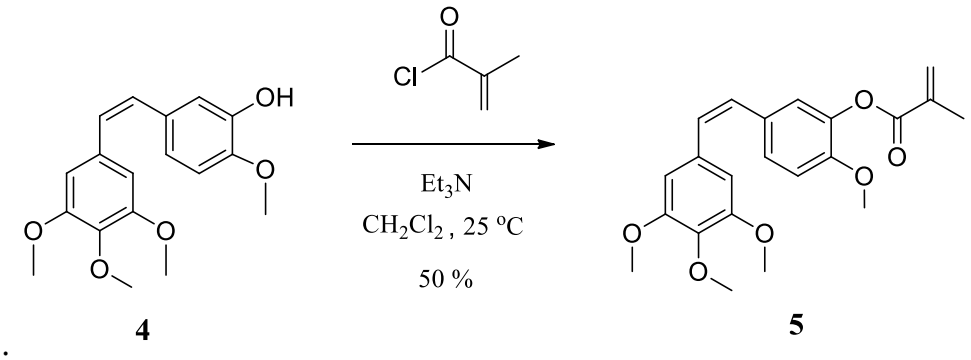

Figure 3.6. Synthesis of ester linked drug monomer, CA4-MA (**5**).

In Figure 3.7 ^{1}H NMR characterization of compound **5** is illustrated. The indication of attachment of methacrylate unit to the drug molecule is the singlet peaks at 5.69 and 6.29 ppm (peak e in Figure 3.7) and at 2.00 ppm (peak d in Figure 3.7). Moreover,

disappearance of hydroxy peak of CA4 at 5.50 ppm indicated the conjugation of methacrylate from hydroxyl group. All other peaks in the spectrum belong to CA4 (**4**). When the spectrum of **5** is compared to that of CA4 (**4**, Figure 3.4), the protons of compound **4** have been shifted to down field after carbonyl conjugation.

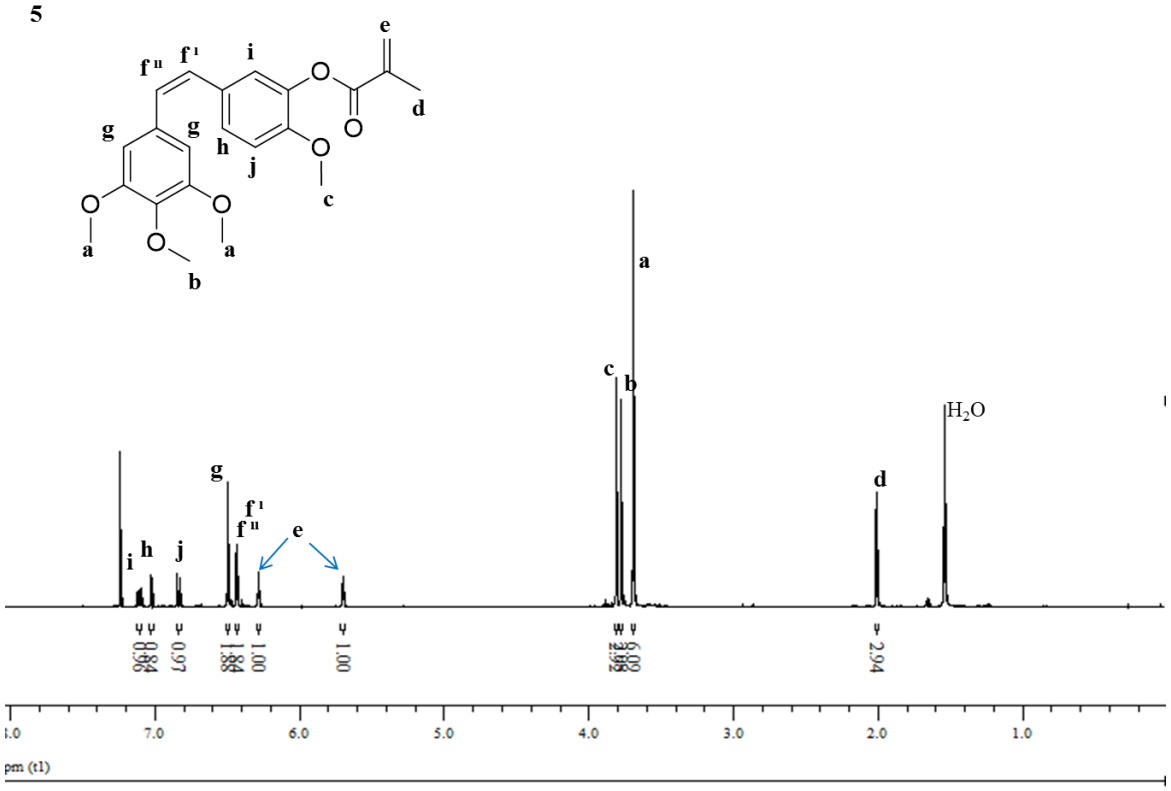

Figure 3.7. ^{1}H NMR spectrum of compound **5**.

In Figure 3.8, the FT-IR spectrum of CA4 (**4**) is compared to that of CA4-MA (**5**). It can be easily seen that hydroxyl stretching of CA4 at 3288 cm^{-1} (peak A) has disappeared after attachment of methacrylate. The carbonyl group in the monomer (**5**) has a sharp peak at around 1739 cm^{-1}. The C-C double bond stretching of methacrylate group in CA4-MA at 1677 cm^{-1} is the main indication of formation of the co-monomer **5**. Besides, C-C double bond stretching between two aromatic rings in the monomer (**5**) is still observed at 1577 cm^{-1}.

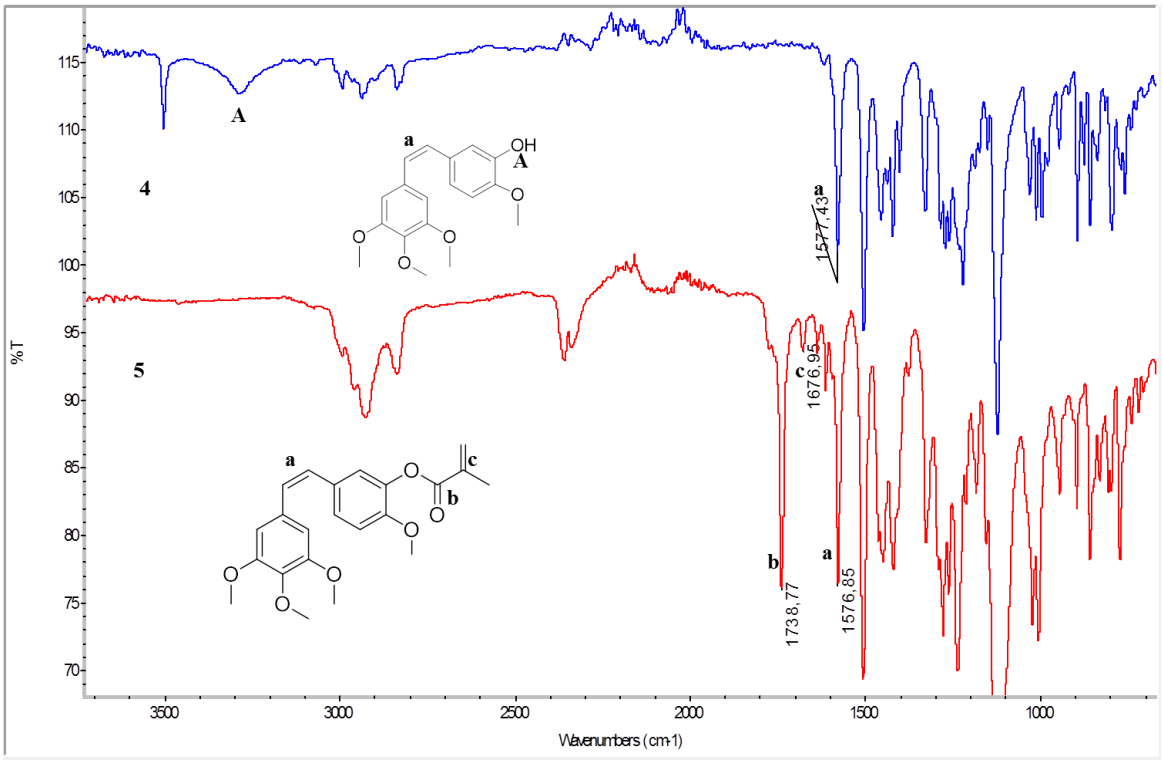

Figure 3.8. FT-IR spectrum comparison of compound 5 to 4.

The ester linked drug monomer was copolymerized with highly water soluble Poly(ethylene glycol) methyl ether methacrylate (PEGMA, M_n = 300 g/mol) via free radical polymerization using AIBN as initiator (Figure 3.9). Since AIBN dissociates to its radical form at about 70 ^oC, the polymerization was started at that temperature. In the first polymerization reaction temperature was descended to 60 ^oC thirty minutes after reaction was started and kept under these conditions for 24 h. By GPC characterization molecular weight of the co-polymer **6a** was found out as 23600 with a M_n/M_w of 1.67 (Table 3.1, item 1). The second polymerization reaction was started at 70 ^oC and kept at this temperature for 24 h. By GPC characterization molecular weight of the co-polymer **6b** was determined as 27600 with an M_n/M_w of 1.63 (Table 3.1, item 2).

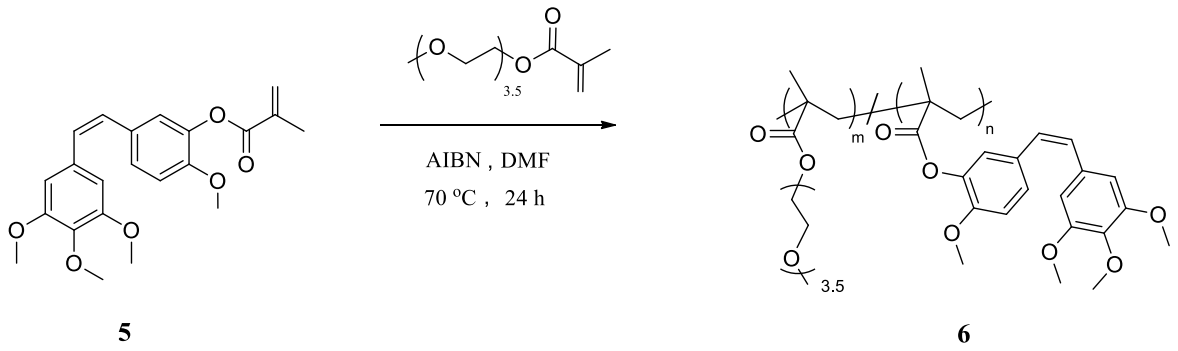

5 **6**

Figure 3.9. Polymerization reaction to produce ester linked drug conjugate (**6**).

After copolymerization of CA4-MA (**5**) with PEGMA via free radical polymerization, purification of polymer (**6**) was achieved by precipitate the product in cold diethyl ether. It could be seen from ^{1}H NMR assignment (Figure 3.10 and 3.11) that free CA4-MA (**5**) monomer was not left over after precipitation. Comparison of spectrum 6a, **6b** to spectrum **5** demonstrates that the peaks at 5.69 and 6.29 ppm (e in Figure 3.7) have disappeared after polymerization.

Table 3.1. Characteristics of polymer-drug conjugates.

No	Polymers	Feed ratio [CA4-MA] :[PEGMA]	Obtained ratio [CA4-MA] :[PEGMA]	M_n (g/mol)	M_w/M_n	% CA4 (w/w)	Conversion (%)
1	**6a**	1 : 10	1 : 15	23600	1.67	6.5	60
2	**6b**	1 : 4	1 : 11	27600	1.63	8.6	80

According to Table 3.1, obtained monomer ratio [CA4-MA]:[PEGMA] for polymer **6a** is 1 : 15 and for polymer **6b** it is 1 : 11. They were determined after their ^{1}H NMR characterizations (Figure 3.10 and 3.11). CA4 percent (w/w) in the conjugates was also calculated by integration on ^{1}H NMR spectra.

For the obtained monomer ratio [CA4-MA] : [PEGMA] in polymer **6a**, peak a represented 3 protons of methoxy units of PEGMA side chains at 3.35 ppm and the peak at 6.45 ppm protons b, c, d (Figure 3.10) were integrated . Then the integrated value of peak a was divided by 3 and that of peak b,c,d was divided by 4. The results were indicated [CA4-

MA] : [PEGMA] ratio as 1 : 15. Another calculation determined the CA4 percent (w/w) in polymer 6a as 6.5 %.

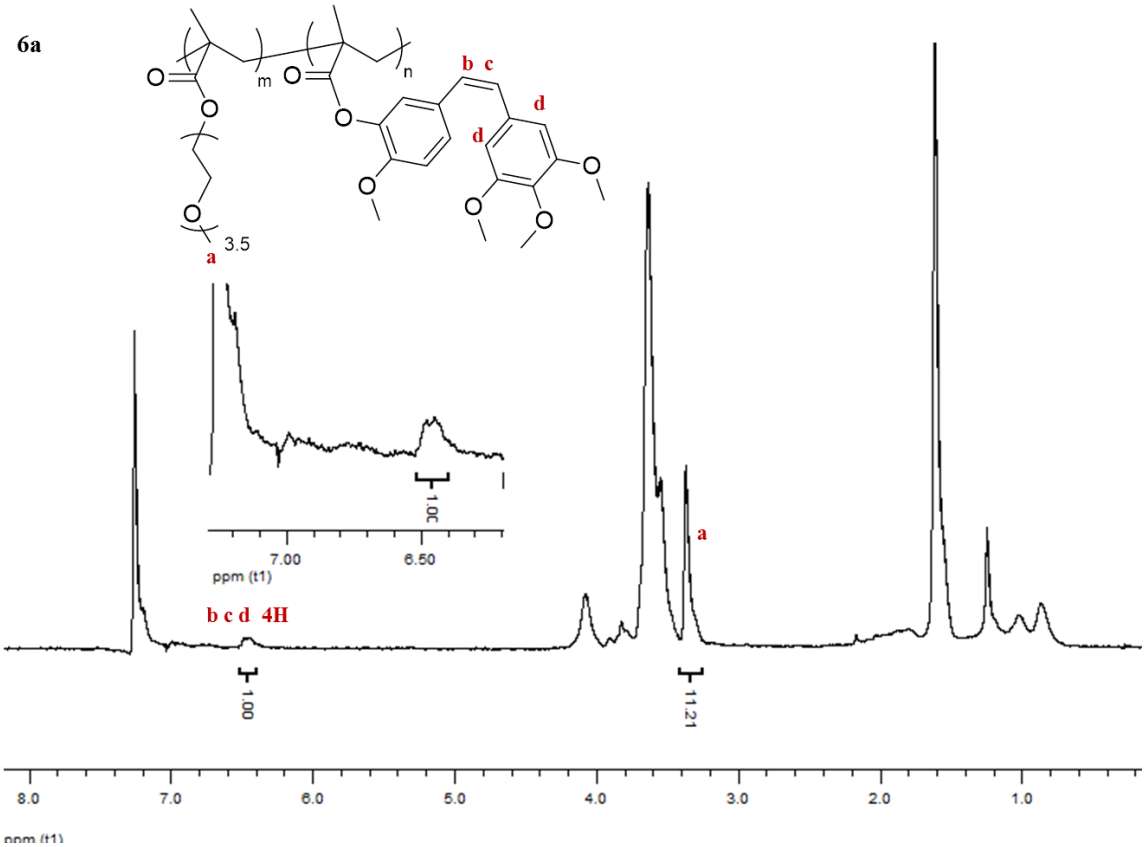

Figure 3.10. ^{1}H NMR spectrum of copolymer **6a** with 6.5 % CA4.

^{1}H NMR characterization of compound 6b also demonstrates the obtained monomer ratio [CA4-MA] : [PEGMA] as 1 : 11. This ratio is calculated by integration of the peaks c and a (Figure 3.11). As mentioned above, the peak a represents the 3 protons of methoxy unit in PEGMA. When its integration value 32.87 is divided by numbers of protons 3, it is obtained that PEGMA units in the copolymer **6b** are 11 times to CA4-MA units. The obtained ratio also gives the CA4 weight percent in the polymer as 8.6 %.

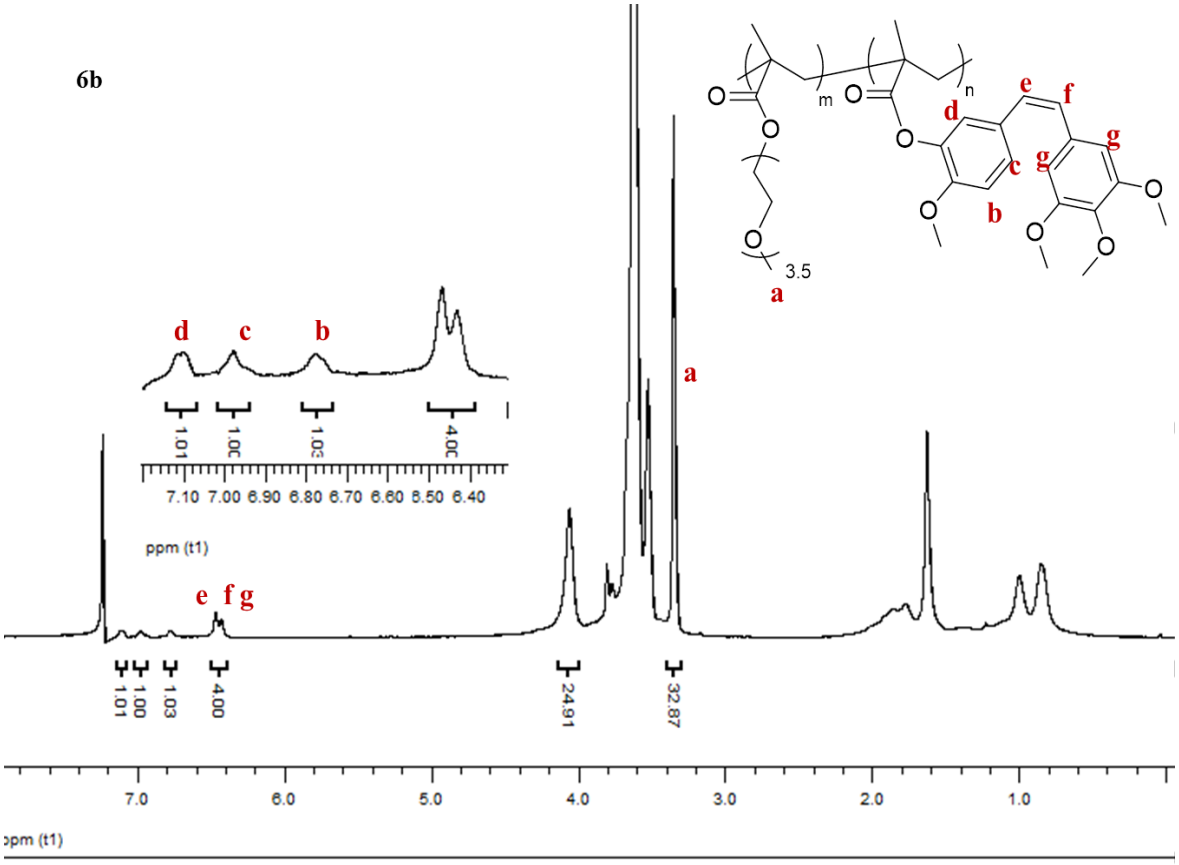

Figure 3.11. ^{1}H NMR spectrum of copolymer **6b** with 8.6 % CA4.

By light scattered GPC characterization their molecular weights and polydispersities were discovered (M_w/M_n, M_n Table 3.1). Even though polydispersity values of both conjugate are much higher than 1, there is no polymer with molecular weight higher than 35 kDa inside compounds. Since a linear copolymer with nondegradable backbone can go through renal clearance if the molecular weight is less than 50 kDa, the constructs 6 a and 6 b can be removable from the body.

The characterization of co-poly-(CA4MA-PEGMA) was also done by FT-IR and compared to CA4-MA (**5**). As displayed in Figure 3.8 the peak at 1677 cm^{-1} due to C-C double bond stretching of methacrylate group in compound **5** disappeared after polymerization. A broad and strong peak at around 2871 cm^{-1} in the spectrum of co-poly-(CA4MA-PEGMA) is observed because of C-H stretching of polymer backbone. Besides, internal C-C double bond stretching of CA4-MA at 1577 cm^{-1} can still be seen at 1580 cm^{-1} after formation of copolymer.

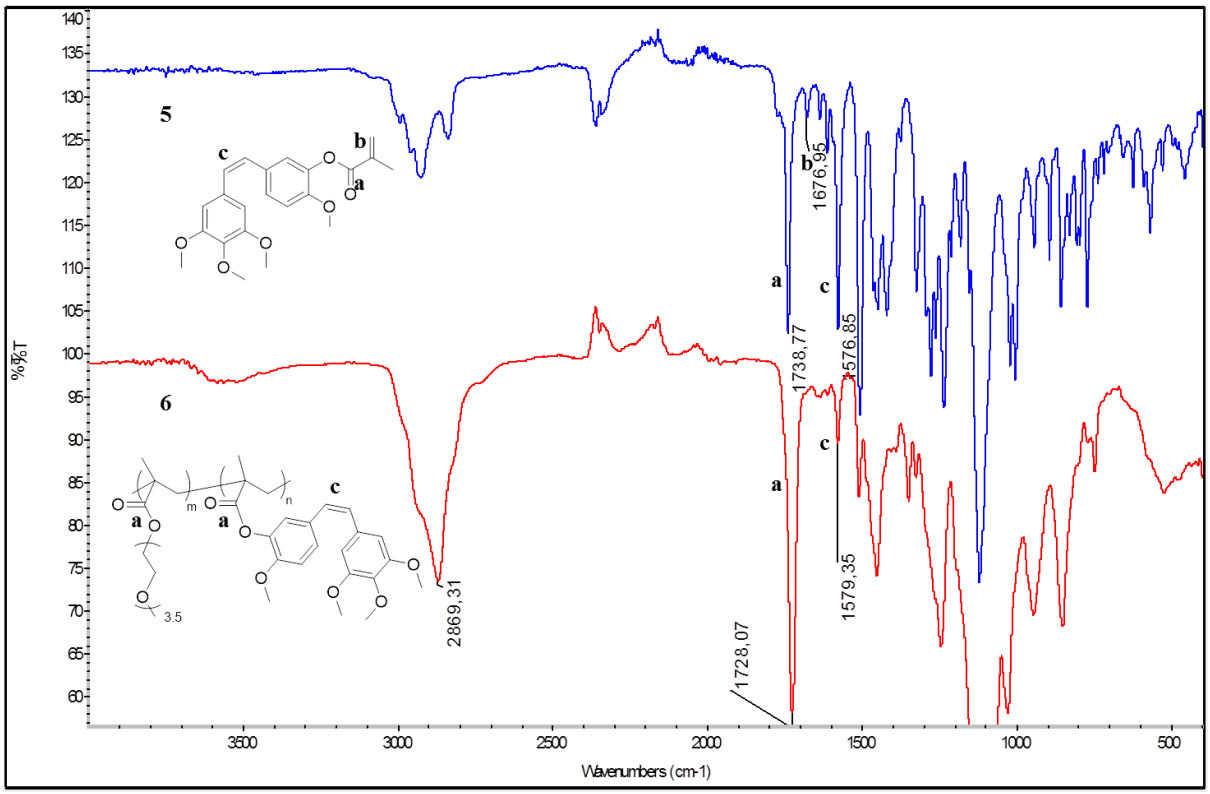

Figure 3.12. FT-IR comparison of **5** and **6**.

.

3.2. In Vitro Evaluation of the Conjugates

3.2.1. Stability of CA4

Stability of CA4 in acidic (pH 4.8), neutral (pH 7.4) and basic (pH 10.0) media was investigated so that it is understood if all CA4 at the beginning still remain in the medium or it gets degraded within time. This profile will be helpful for further *in vitro* experiments. These studies were undertaken only once and hence needs further optimization.

3.2.2. Cell Viability and Cytotoxicity Assay

To compare anti-proliferation activity of free CA4 and polymeric conjugate with 8.6 % CA4 (**6b**), HUVECs in endothelial cell complete media were exposed to a series of equivalent concentrations of CA4 with drug itself and with drug in polymeric conjugate (6b) for 48 h. The concentration of CA4 in the conjugate that cause 50 % cell death was

much lower than that of free drug (Figure 3.14, EC_{50}=2.4 nM vs 7.5 nM). The difference is probably due to slow release of CA4 in HUVECs. Even though CA4 is more effective on anti-proliferation of the cells this advantage of CA4 cannot be achieved *in vivo* due to its broad distribution in normal tissues. Hence, these results indicate that conjugation of CA4 to highly water soluble polymer via ester linkage can enhance the anti-proliferation activity of CA4 on endothelial cells.

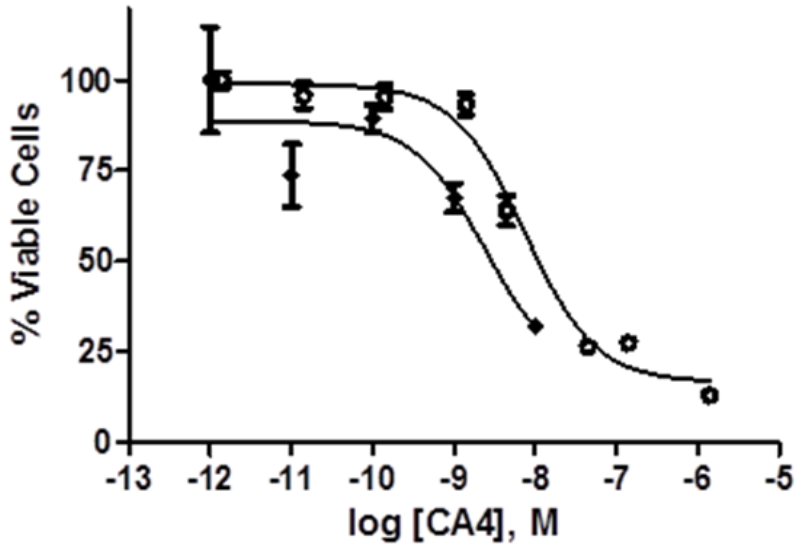

Figure 3.13. The viability of HUVECs exposed to free CA4 (♦) and polymeric conjugate **6b** (○).

4. EXPERIMENTAL

4.1. General Methods and Materials

All chemicals were purchased from manufacturer Alfa Aesar, Aldrich, Bachem, and Merck. Methanol from Prolabo was used as procured. DMF from Aldrich and CH_2Cl_2 from Merck were dried over molecular sieves. All other solvents were used without any further purification. Column chromatography was performed using silicagel-60 (43-60 nm). Liquid Chromatography-Mass Spectrometry (LC-MS) analysis was performed with Schimadzu LCMS 2020 with ACN-Water eluent mixture. Preparative High Pressure Liquid Chromatography (prep HPLC) analysis for purification was carried out on Schimadzu LC-6 AD with ACN and water as eluents. Characterizations of monomers and copolymers were done by ^{1}H NMR Spectroscopy (Varian Mercury 400 MHz) in $CDCl_3$ and DMSO-d_6 and Fourier Transform Infrared (ATR-FT-IR) Spectroscopy (Thermo Fisher Scientific Inc. Nicolet 380). Molecular weights of conjugates were determined by Gel Permeation Chromatography (GPC) analysis using Shimadzu GPC furnished with a PSS-SDV (length/ID 8 × 300 mm, 10 mm particle size) mixed-C column calibrated with polystyrene standards (1–150 kDa) using a refractive-index detector.

Cell viability experiments with the conjugates were performed on Human umbilical vein endothelial cell (HUVEC) which were purchased from Lonza Group Ltd. and maintained in EGM-2 complete medium in a humidified atmosphere at 37 °C and 5 % CO_2.

4.2. Synthesis of Drug Monomers

4.2.1. Synthesis of Combretastatin A4

4.2.1.1. Synthesis of E-2-(3',4',5'-Trimethoxyphenyl)-3-(3'-hydroxy-4'-methoxyphenyl) prop-2-enonic acid. E-2-(3',4',5'-Trimethoxyphenyl)-3-(3'-hydroxy-4'-methoxyphenyl) prop-2-enonic acid (**3**) was synthesized according to the procedure on literature [25]. 3-hydroxy-4 methoxybenzaldehyde (0.61 g, 4.4 mmol), 3,4,5-trimethoxyphenylacetic acid (1g, 4.4 mmol), acetic anhydride (1.3 mL) and triethylamine (2 mL) mixture was heated under reflux at 160 °C for 3 h. The product was acidified with 3 mL concentrated hydrochloric acid. After waiting for overnight, the solid formed was filtered off and recrystallized from ethanol to give propenonic acid (**3**) (0.9 g, 64 %) as fine yellow crystals. FT-IR (cm^{-1}); 3323, 1663, 1610, 1583, 1501.

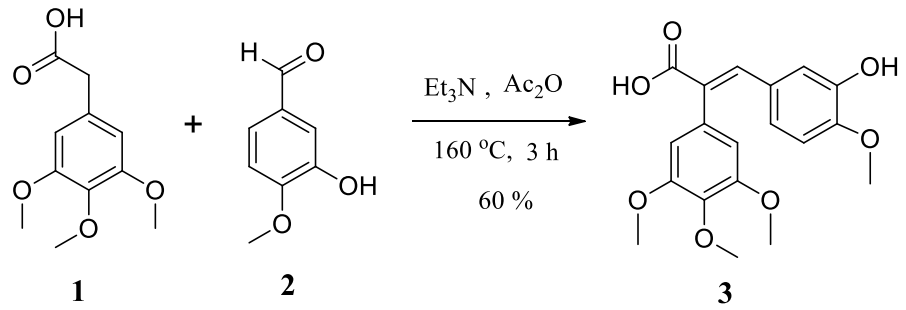

Figure 4.1. Synthesis of propenonic acid (**3**).

4.2.1.2. Synthesis of Combretastatin A4 by Decarboxylation of Propenonic Acid. Combretastatin A4 (**4**) was synthesized according to the literature procedure [25]. To a solution of (Z)-3-(3'-Hydroxy-4'- methoxyphenyl)- 2-(3'',4'',5''-trimethoxyphenyl)prop-2-enoic acid (3) (0.36 g, 1.00 mmol) in quinoline (1.5 mL, 1.8 g, 0.014 mol) was added powdered copper (0.35 g, 5.48 mmol), and then the reaction mixture was refluxed at 210 °C. After 3 h of reaction time, the mixture was cooled. Subsequently, ether was added to cooled reaction mixture, and the powdered copper was filtered off through Celite. The ether layer (filtrate) was washed with 1 M hydrochloric acid. Then the organic layer was separated and the aqueous layer was extracted with more ether. The combined organic layers were washed with saturated aqueous sodium carbonate (3 x 20 mL), water (3 x 20

mL), brine (2 x 20 mL), dried over Na_2SO_4, and concentrated in *vacuo*. Crude mixture was purified via column chromatography (ethyl acetate : hexane, 5 : 95) and pure CA4 was obtained as pale yellow crystals (0.09 g, 30 % yield). ^{1}H NMR($CDCl_3$, δ, ppm); 6.9 (d, *J* = 2 Hz, 1H, CH=COH), 6.8 (dd, *J* = 8,4 Hz, *J* = 2 Hz, 1H, CH-C- CH=COH), 6.71 (d, *J* = 8,4 Hz, 1H, CH=C-C-OH), 6.56 (s, 2H,CH=C-CH), 6.42 (d, *J* = 12.4, 2H, CH=CH), 5.50 (s, 1H OH-C=CH) 3.85 (s, 3H, CH_3-OC-COH), 3.82 (s, 3H, CH_3O-C-CO CH_3), 3.68 (s, 6H, CH_3O-C-C-OCH_3=C-OCH_3). FTIR (cm^{-1}); 3288, 1577, 1504.

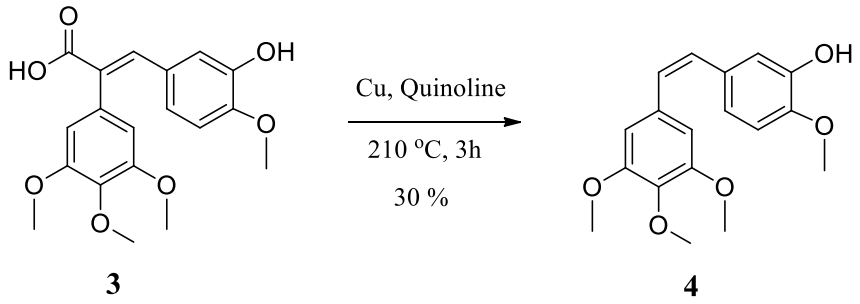

3 **4**

Figure 4.2. Synthesis of Combretastatin A4 (**4**).

4.2.2. Synthesis of Drug Monomer with Ester Linker

To a solution of compound **4** (0.04 g, 0.13 mmol) in CH_2Cl_2 (2.5 mL), triethylamine (35 µL, 0.25 mmol) was added. To that mixture at 0 °C was added methacrylolyl chloride (13.5 µL, 0.14 mmol) in CH_2Cl_2 (1 mL) dropwise over 10 minutes. The reaction mixture was stirred for 24 h at room temperature under dry condition. Upon the reaction complete, CH_2Cl_2 (2.0 mL) was poured in the mixture and the organic phase was extracted with saturated $NaHCO_3$ (2 x 20 mL) and H_2O (2 x 20 ml). Combined organic layers were dried over anhydrous Na_2SO_4 and concentrated to give a yellowish solid which was purified by column chromatography on SiO_2 (EtOAc : Hexane 5 : 95) affording 0.025 g (51%) CA4-MA monomer (**5**) ^{1}H NMR ($CDCl_3$, ppm); 7.11 (dd, *J*= 8.4 Hz *J*= 2 Hz, 1 H, CH=C-CH=CO-), 7.03 (d, *J*= 2 Hz, 1 H, CH=C-OCH_3-CO-), 6.84 (d, *J*= 8.8 Hz, 1 H, CH=CO-), 6.50 (s, 2H, CH=C-CH), 6.44 (d, *J*= 3.2 Hz, 2 H, CH=CH), 6.28 (s, 1 H, HC=C-CH_3), 5.70 (s, 1 H, HC=C-CH_3), 3.81 (s, 3 H, CH_3O-C=CO-), 3.78 (s, 3 H,

CH3O-C=C-CH), 3.69 (s, 6 H, CH_3OC=C-OCH_3-$COCH_3$), 2.01 (s, 3 H, CH_3-C=C-). FT-IR (cm^{-1}); 1739, 1677, 1577.

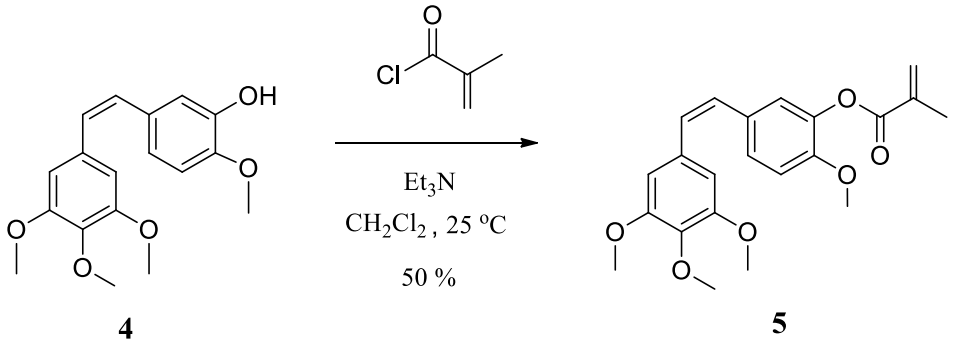

4 **5**

Figure 4.3. Synthesis of CA4-MA (**5**).

4.2.3. Ester Linked Polymer Drug Conjugate Synthesis

The polymer drug conjugate, co-poly(CA4MA-PEGMA) (**6**) was synthesized through free radical polymerization using AIBN as initiator. To a solution of compound **5** (35 mg, 0.09 mmol) in DMF (3 mL) was added PEGMA (104 µL, 0.36 mmol under $N_{2(g)}$. In a separate vial AIBN (0.53 mg, 3.25 x 10^{-3} mmol) was dissolved by DMF (1 mL) and purged under $N_{2(g)}$. The monomer solution was heated to 70 ^oC in an oil bath and AIBN solution was added to the mixture. The reaction mixture was stirred for 24 h at 60 ^oC to obtain polymer **6a** and at 70 ^oC to obtain polymer **6b**. 24 h later the reaction temperature was cooled to room temperature and polymerization was terminated. DMF was evaporated and the crude mixture was precipitated in cold diethyl ether. The precipitate was filtered and dried under *vacuo*. The copolymer **6** was washed with diethyl ether at room temperature after first filtration and then precipitated in cold diethyl ether again. GPC characterization gave co-poly(CA4MA-PEGMA) **6a** has molecular weight of 23 K with M_w/M_n of 1.63 and **6b** has molecular weight of 27.6 K with M_w/M_n of 1.67. ^{1}H NMR ($CDCl_3$, ppm); 7.10 (d, *J*= 7.66 Hz, 1 H, CH=C-CH=CO-), 6.98 (s, 1 H, CH=C-OCH_3-CO-), 6.78 (s, 1 H, CH=CO-), 6.45 (d, *J*= 14 Hz, 4H, CH=C-CH and bridged CH=), 4.06 (br s, 4 H, COO-CH_2), 3.81 (s, 3 H, CH_3O-C=C-C-OCH_3), 3.77 (s, 3 H, CH_3O-C=CO-), 3.63 (br s, 20 H, -CH_2CH_2O- and CH_3OC=C-OCH_3-$COCH_3$), 3.53 (br s, 2 H, -CH_2CH_2O-), 3.35 (s, 3H, CH_3O-CH_2CH_2-), 1.99-0.75 (m, CH_2 and CH_3 along with backbone). FT-IR(cm^{-1}); 1728, 1580.

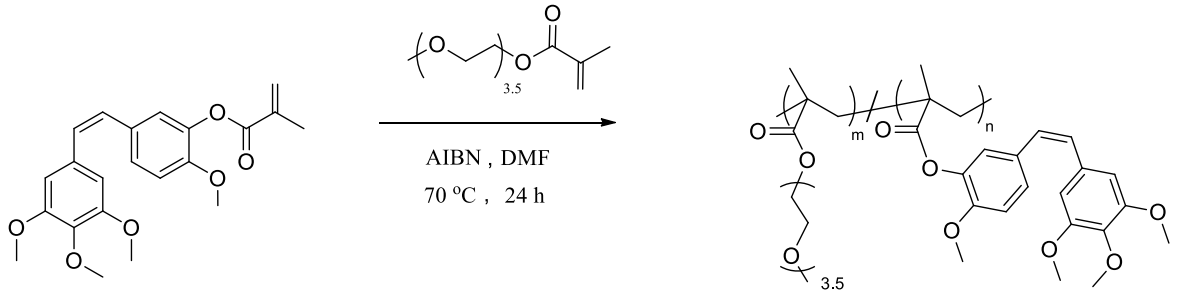

5 **6**

Figure 4.4. co-poly(CA4MA-PEGMA) Synthesis.

4.2.4. In Vitro Evaluations of Drug Conjugates

4.2.4.1. CA4 Stability. CA4 (0.223 mg) was dissolved in DMSO (223 µL) to prepare 1mg/mL solution of CA4. Subsequently, CA4 solution (10 µL/sample) was separated into 21 different tubes containing 190 µL acetate buffer solution (pH 4.8, NaAc/HAc) in 7 tubes, 190 µL PBS solution (0.1 M phosphate buffer in 0.05 M NaCl at pH 7.4) in other 7 tubes and 190 µL glycine buffer (0.2 M glycine buffer in 0.2 M NaOH at pH 10) in the rest 7 tubes. All the tubes including 0.05 mg/mL CA4 were incubated at 37 °C. Then the samples from each media were removed at time 0 min, 1 h, 2 h, 6 h, 12 h, 24 h and 48 h. The aliquots were immediately placed in the freezer. At the end of the 48 h, all the tubes were filled by 300 µL Acetonitrile and analyzed using LC/MS via 50-95 (gradient ACN) LC & SIM317 MS method and compared to calibration standards prepared using serial dilutions of CA4 in ACN phase. Finally concentration in each tube was determined.

4.2.4.2. Cell Viability and Cytotoxicity Assay. In this assay, the water soluble WST-8 (2-(2-methoxy-4-nitrophenyl)-3-(4-nitrophenyl)-5-(2,4-disulfophenyl)-2H-tetrazolium, monosodium salt) dye was reduced by mitochondrial dehydrogenase enzymes in the viable cells to form water soluble formazan dye. Cells were cultured as 2000 or 3000 cells/well in 96-well plates and allowed to recover for 24 hours. Cells were treated with the indicated concentrations of drug conjugates in EGM-2 complete media. After the indicated treatment durations, 10 µL of CCK-8 labeling reagent and 100 µL complete media were added to each well and incubated for 4 hours at 37°C. The absorbance was recorded in a Thermo

Scientific Multiskan FC microplate reader at 450 nm and results were analyzed via SkanIt software. Absorbance values of treatment groups were calculated as percentages of absorbance obtained from Control cells and results were plotted using GraphPad Prism 5 software.

5. CONCLUSION

Novel monomer bearing an anti-angiogenic inhibitor, CA4 was synthesized successfully. Free radical polymerization of the new monomer with highly water soluble and biocompatible PEGMA was achieved. As expected, cell viability profile of the drug conjugates on HUVECs indicated that they are much less toxic than free CA4. It was clearly observed that CA-4 itself is almost 4 fold more toxic than our construct. Considering the slow release profile *in vitro*, it may be concluded that this polymeric conjugate holds promise as a controlled drug delivery agent.

APPENDIX A

^{1}H NMR and FT-IR spectra of the synthesized compounds and GPC result of the polymers are included.

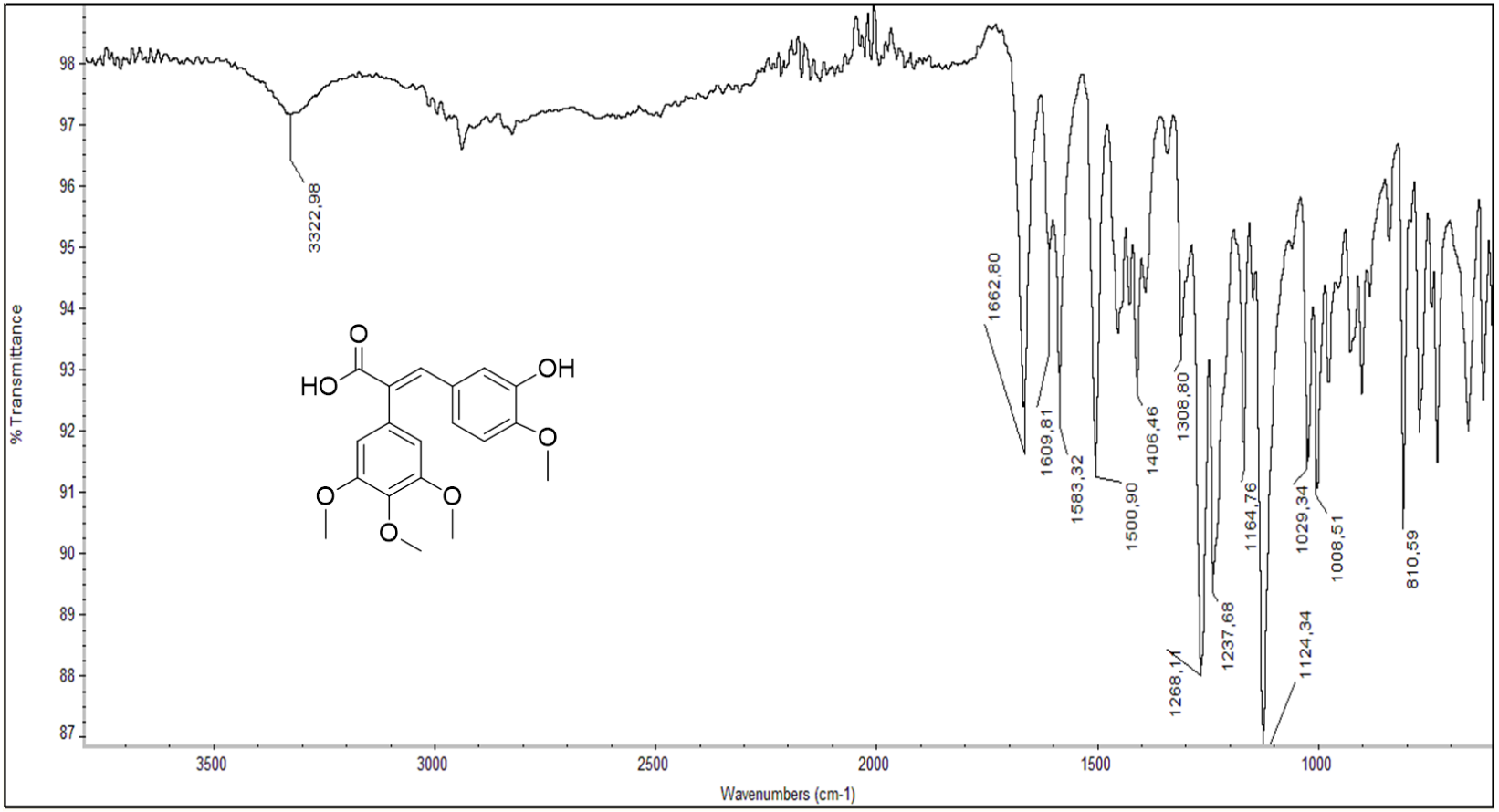

Figure A.1. FT-IR Spectrum of compound 3.

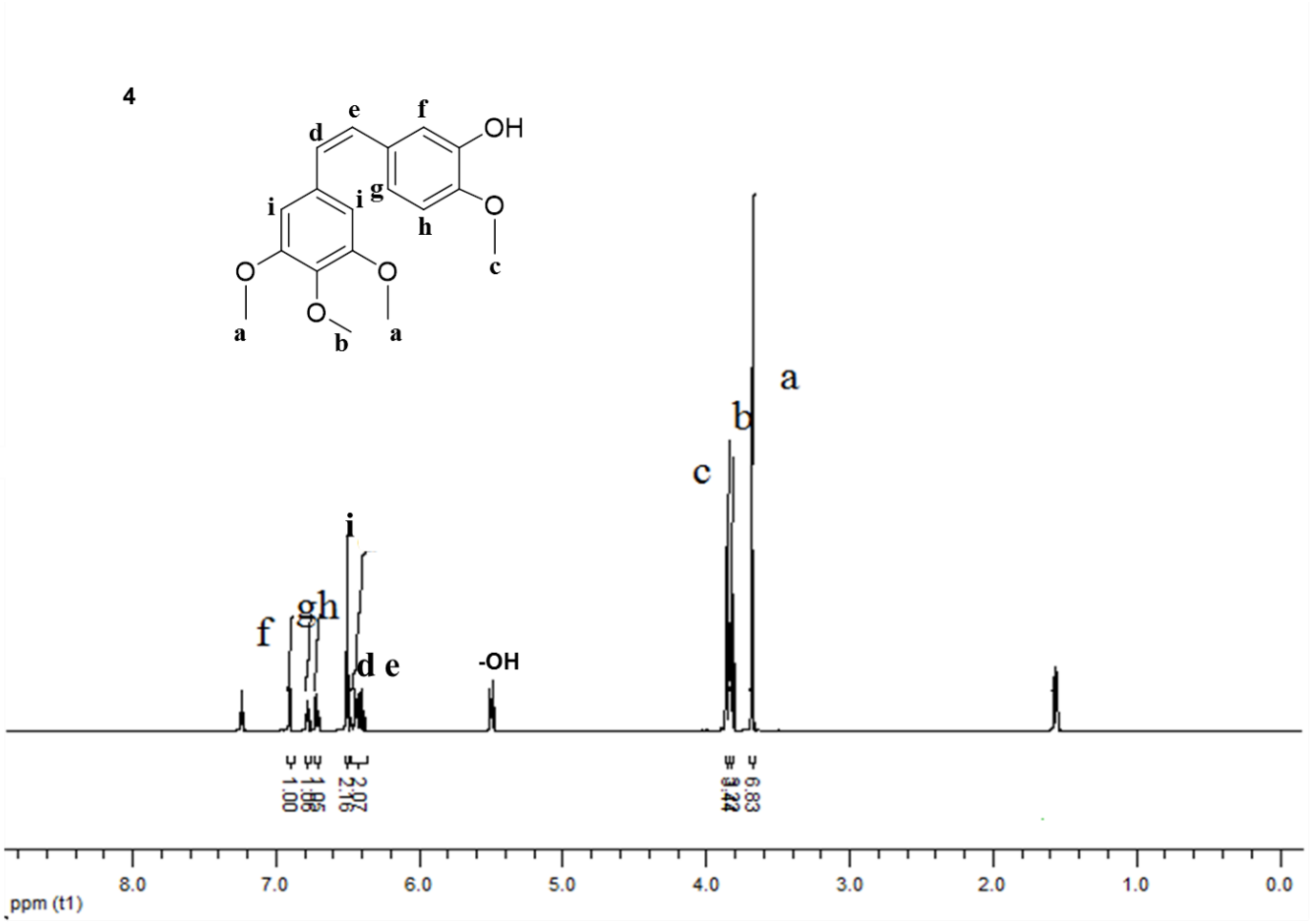

Figure A.2. ^{1}H NMR Spectrum of compound 4.

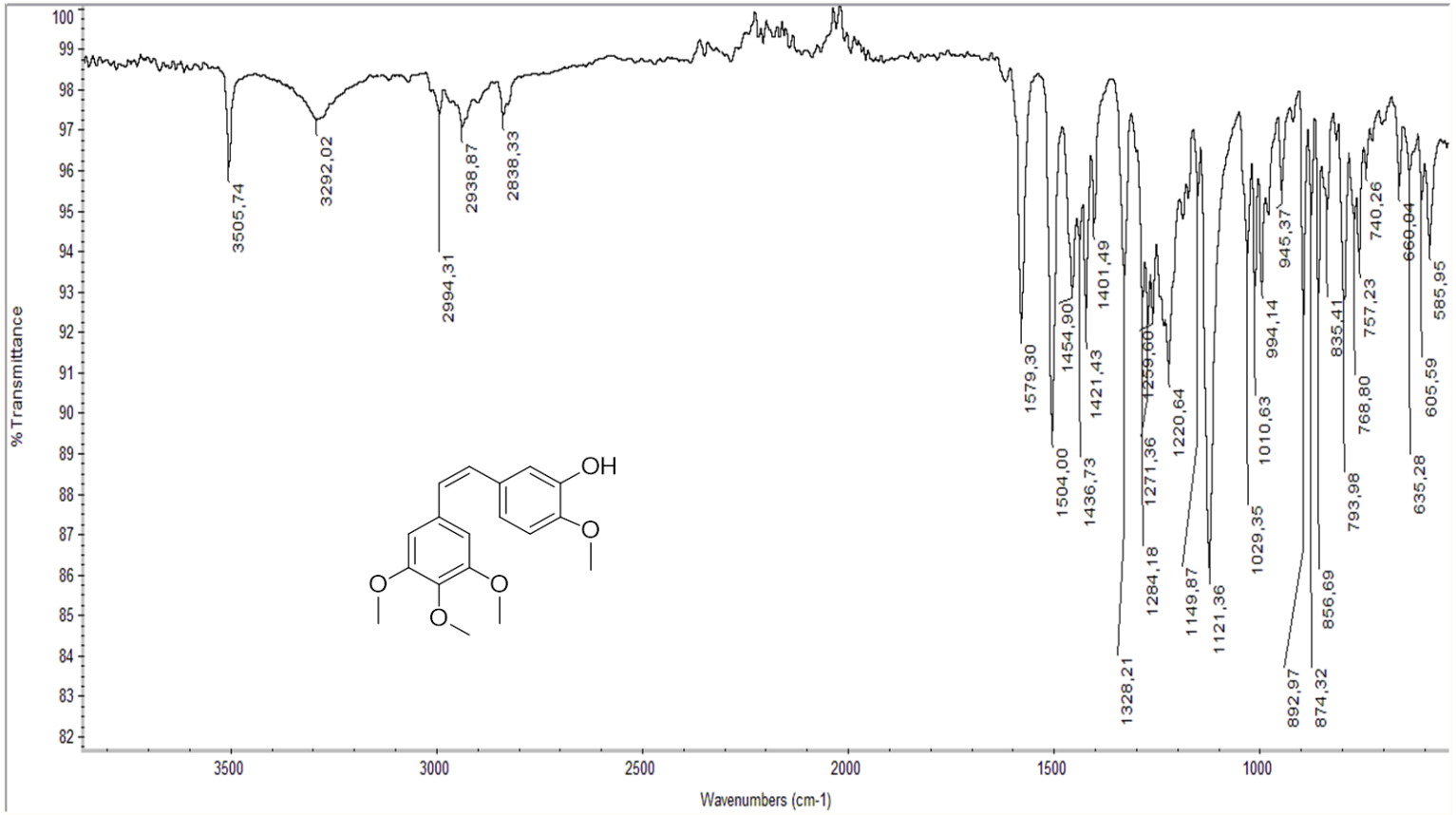

Figure A.3. FT-IR Spectrum of compound 4.

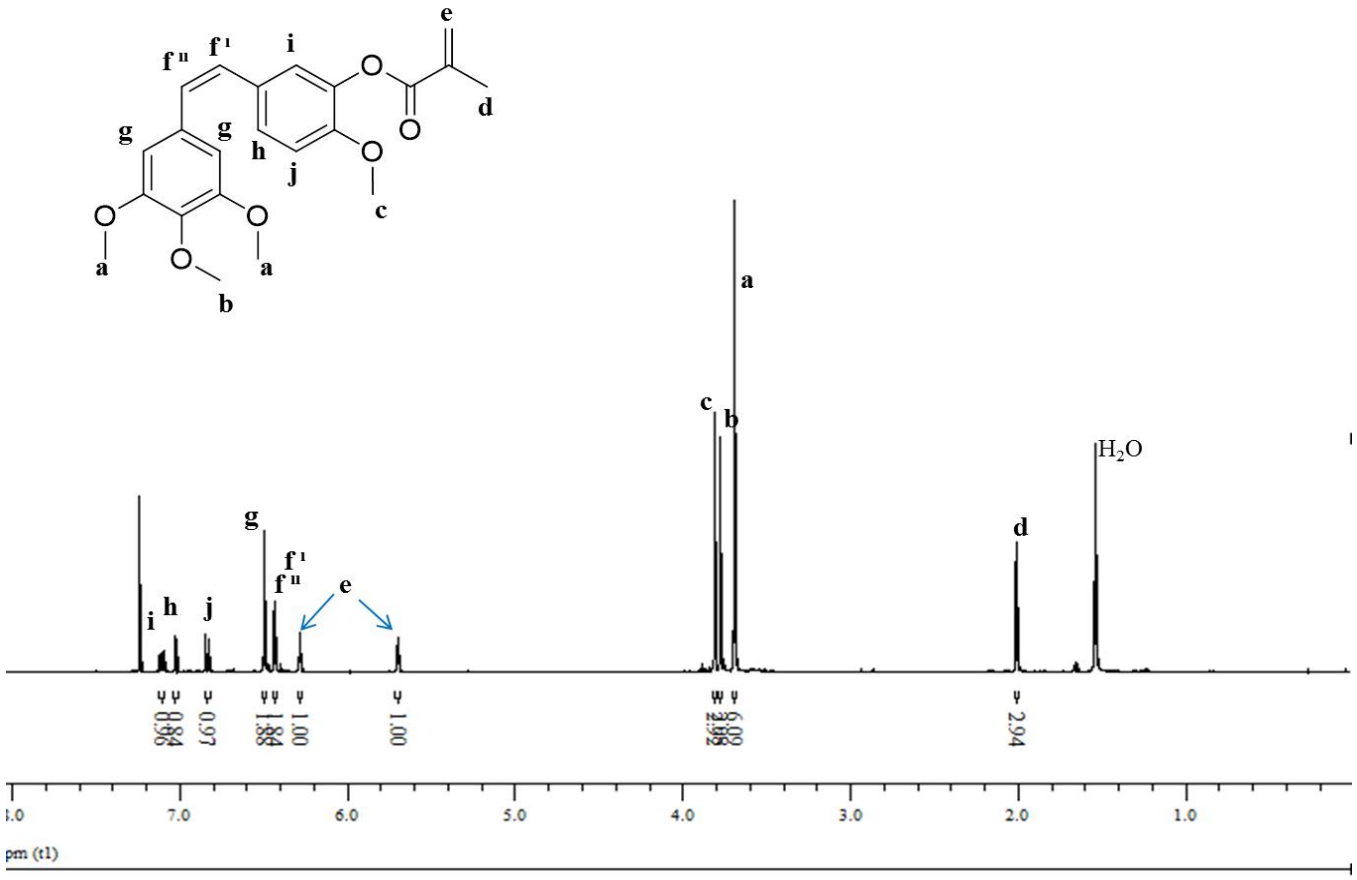

Figure A.4. ^{1}H NMR spectrum of compound 5.

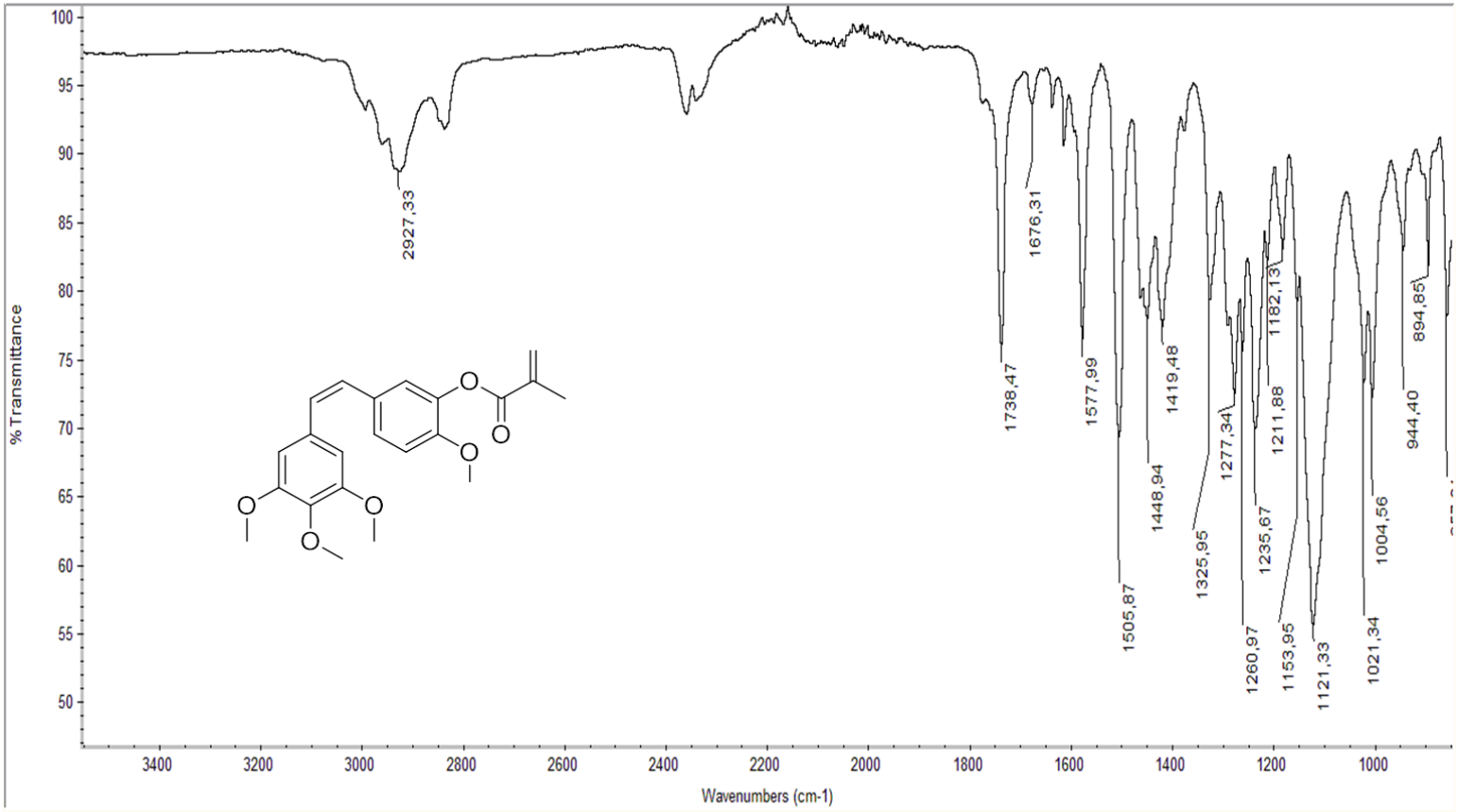

Figure A.5. FT-IR Spectrum of compound 5.

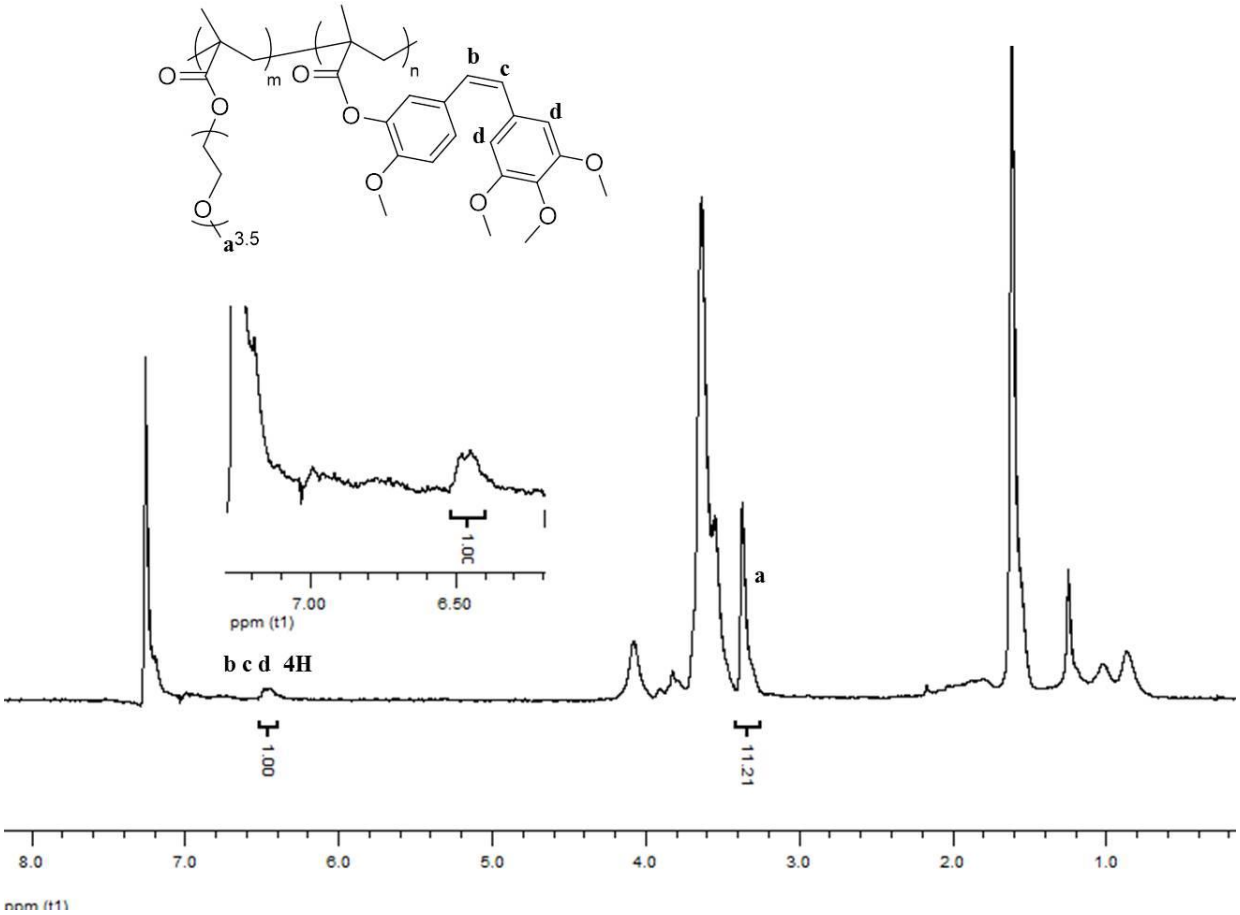

Figure A.6. ^{1}H NMR Spectrum of compound 6a.

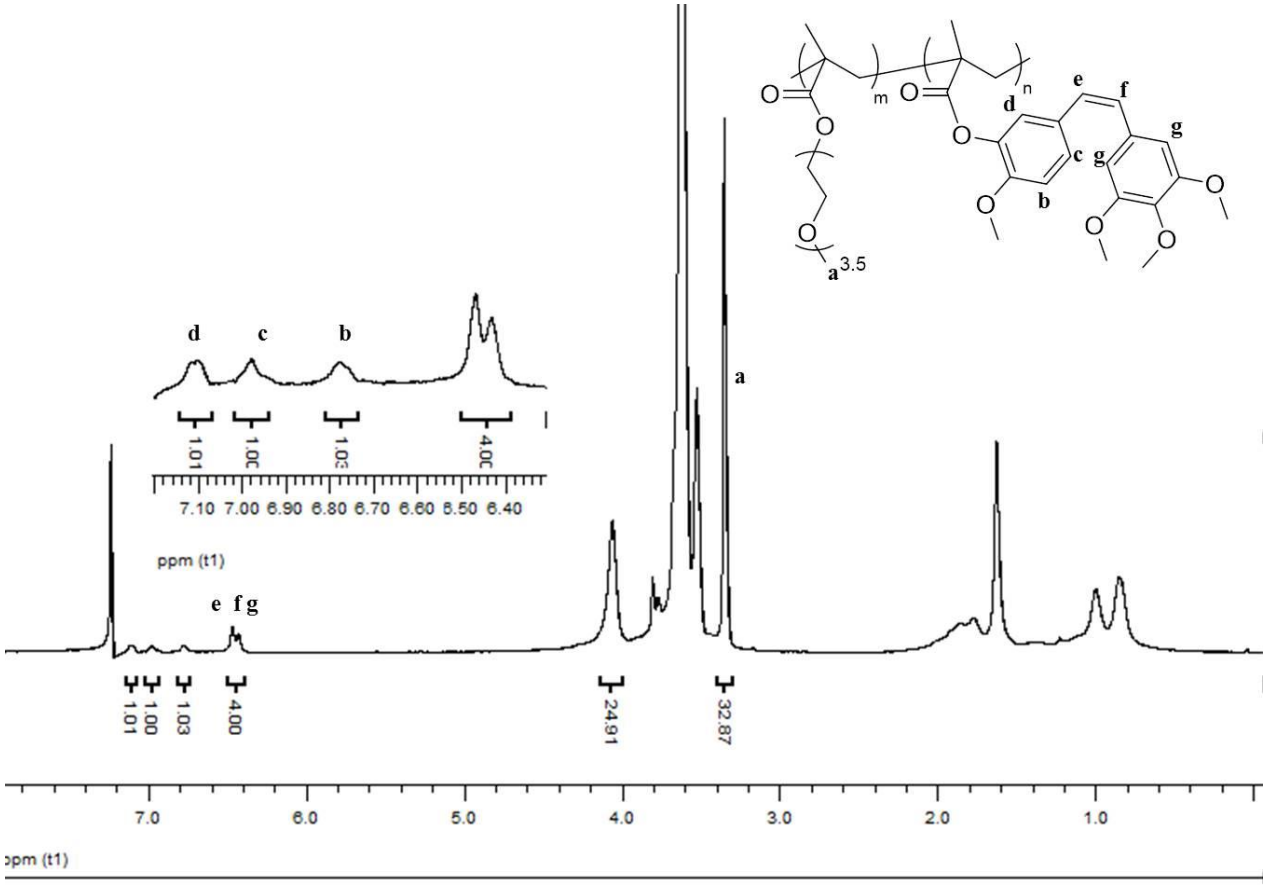

Figure A.7. ^{1}H NMR Spectrum of compound 6b.

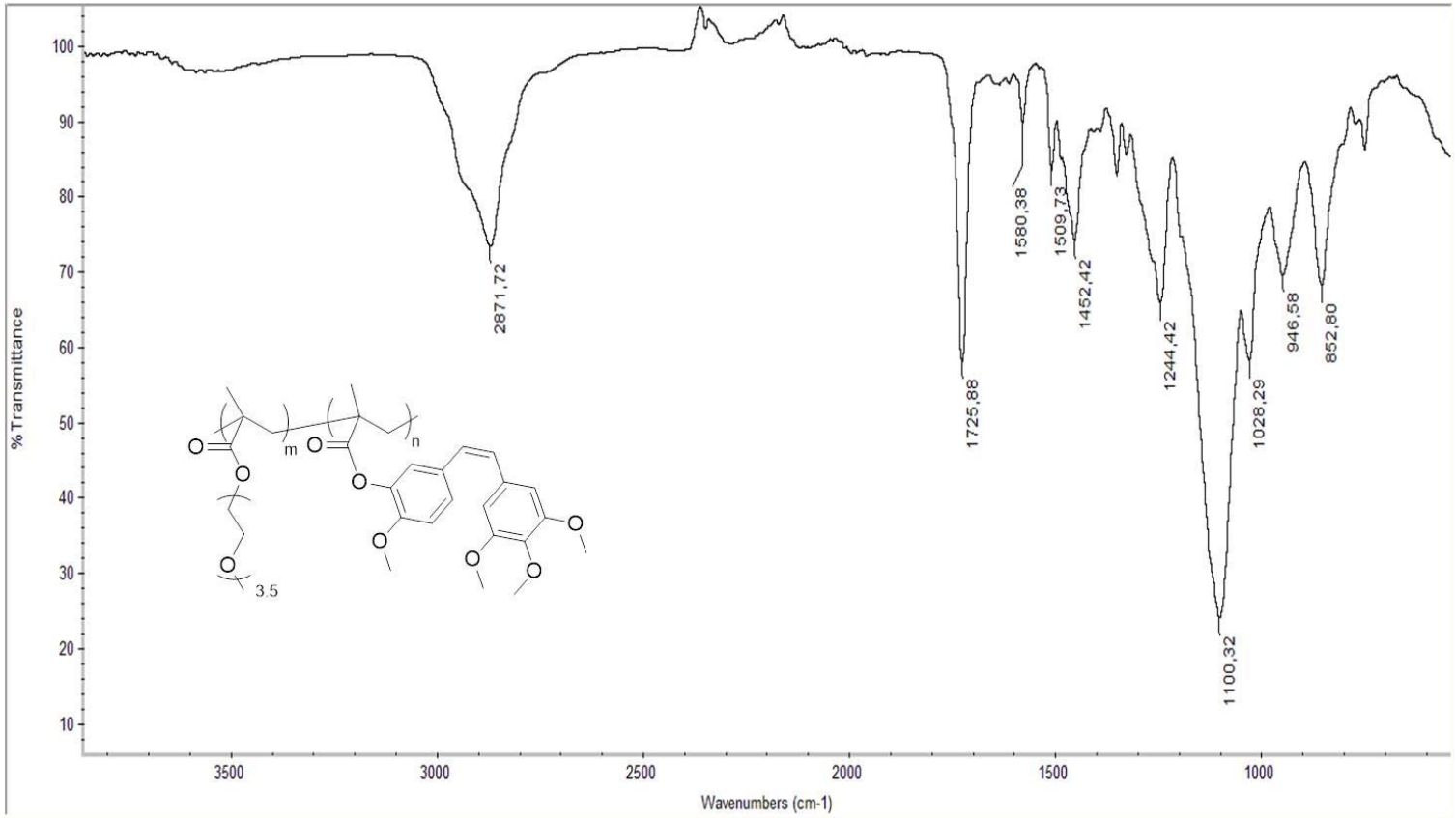

Figure A.8. FT-IR Spectrum of compound 6.

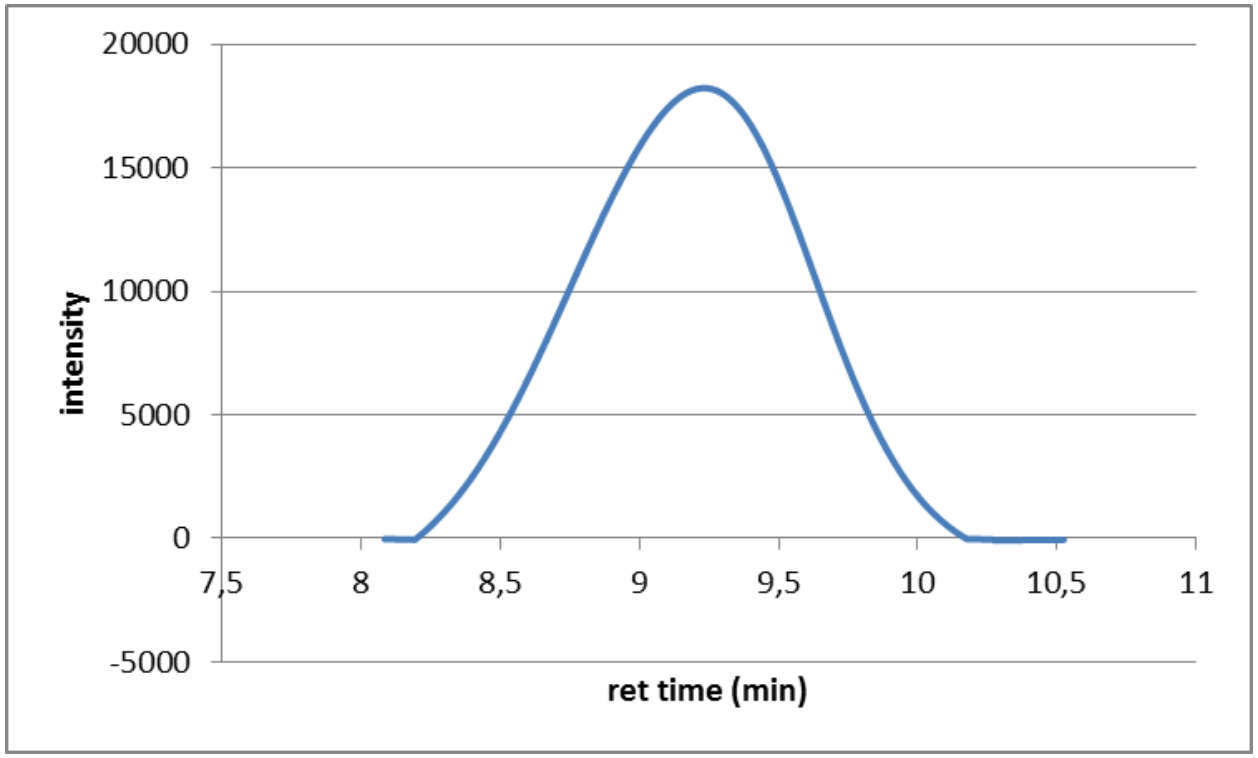

Figure A.9. GPC result of compound 6a.

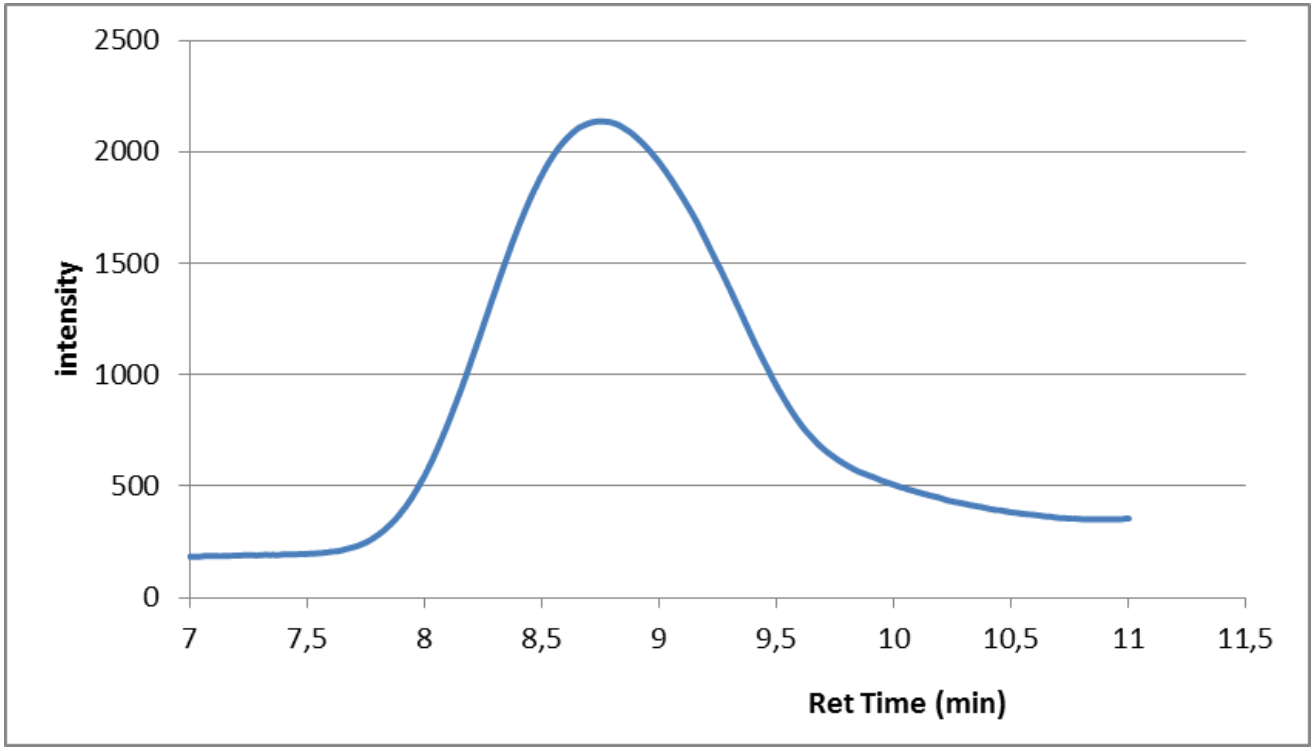

Figure A.10. GPC result of compound 6b.

REFERENCES

1. Sarkar, F. H., S. Banerjee, and Y. Li, "Pancreatic Cancer: Pathogenesis, Prevention and Treatment", *Toxicology and Applied Pharmacology*, Vol. 224, pp. 326-336, 2006.

2. Kleinsmith, L. J., J. Kelly, B. Hollen, "National Cancer Institute", 2009, http://www.cancer.gov/cancertopics/understandingcancer/cancer, July 2013.

3. Fox M. E., F. C. Szoka, and J. M. Fr´echet, "Soluble Polymer Carriers for the Treatment of Cancer: The Importance of Molecular Architecture", *Accounts of Chemical Research*, Vol. 42, No. 8, pp. 1141-1151, 2009.

4. Iyer, A. K., G. Khaled, J. Fang, and H. Maeda, "Exploiting the Enhanced Permeability and Retention Effect for Tumor Targeting", *Drug Discovery Today*, Vol. 11, No. 17/18, pp. 812-818, 2006.

5. Whalen, G. F., and B.R. Zetter, *Angiogenesis, in Wound Healing: Biochemical and Physical Aspects*, I. K. Cohen (editor), Saunders (1992).

6. Danhier, F., F. Olivier, and V. Préat, "To Exploit the Tumor Microenvironment: Passive and Active Tumor Targeting of Nanocarriers for Anti-cancer Drug Delivery", *Journal of Controlled Release*, Vol. 148, pp. 135–146, 2010.

7. Mishra, G. P., N. Duc, and A. W. G. Alani, "Inhibitory Effect of Paclitaxel and Rapamycin Individual and Dual Drug-Loaded Polymeric Micelles in the Angiogenic Cascade", *Molecular Pharmaceutics*, Vol. 10, pp. 2071−2078, 2013.

8. Segal, E., and R. Satchi-Fainaro, "Design and Development of Polymer Conjugates as Anti-angiogenic Agents", *Advanced Drug Delivery Reviews*, Vol. 61, pp. 1159–1176, 2009.

9. Griggs, J., J. C. Metcalfe, and R. Hesketh, “Targeting Tumour Vasculature: The Development of Combretastatin A4”, *Lancet Oncology*. Vol.2, pp. 82–87, 2001.

10. Liekens S., E. D. Clercq, and J. Neyts, “Angiogenesis: Regulators and Clinical Applications”, *Biochemical Pharmacology*, Vol. 61, pp. 253–270, 2001.

11. Wozniak, A., “Challenges in the Current Antiangiogenic Treatment Paradigm for Patients with Non-small Cell Lung Cancer”, *Critical Reviews in Oncology/Hematology*, Vol. 82, pp. 200–212, 2012.

12. Al-Husein, B., M. Abdalla, M., Trepte, D. L. DeRemer, and P. R. Somanath, “Antiangiogenic Therapy for Cancer: An Update”, *Pharmacotherapy*, Vol. 32, No. 12, pp. 1095-1111, 2012.

13. Sun, Y., B. Pandit, S. N. Chettiar, J. P. Etter, A. Lewis, J. Johnsamuel, and Pui-Kai Li, “Design, Synthesis and Biological Studies of Novel Tubulin Inhibitors”, *Bioorganic & Medicinal Chemistry Letters*, Vol. 23, pp. 4465–4468, 2013.

14. Chen, H., Y. Li, C. Sheng, Z. Lv, G. Dong, T. Wang, J. Liu, M. Zhang, L. Li, T. Zhang, D. Geng, C. Niu, and K. Li, “Design and Synthesis of Cyclopropylamide Analogues of Combretastatin-A4 as Novel Microtubule-Stabilizing Agents”, *Journal of Medicinal Chemistry*, Vol. 56, pp. 685−699, 2013.

15. Markovsky, E., H. Baabur-Cohen, A. Eldar-Boock, L. Omer, G. Tiram, S. Ferber, P. Ofek, D. Polyak, A. Scomparin, and R. Satchi-Fainaro, “Administration, Distribution, Metabolism and Elimination of polymer therapeutics”, *Journal of Controlled Release*, Vol. 161 pp. 446–460, 2012.

16. Larson, N. and H. Ghandehari, “Polymeric Conjugates for Drug Delivery”, *Chemistry of Materials*, Vol. 24, pp. 840−853, 2012.

17. Duncan, R., "The Dawning Era of Polymer Therapeutics", *Natural Review Drug Delivery*, Vol. 2, No. 5, pp. 347-260, 2003.

18. Duncan, R., and M. J. Vicent, "Polymer Therapeutics-Prospects for 21st Century: The End of the Beginning", *Advanced Drug Delivery Reviews*, Vol. 65, pp. 60–70, 2013.

19. Kopecek, J., P. Kopeckova´a, T. Minkoa, Z.-R. Lua, and C.M. Petersonc, "Water Soluble Polymers in Tumor Targeted Delivery", *Journal of Controlled Release*, Vol. 74 pp. 147–158, 2001.

20. Maa, P., and R. J. Mumpera, "Anthracycline Nano-delivery Systems to Overcome Multiple Drug Desistance: A comprehensive Review", *Nano Today*, Vol. 8, pp. 313-331, 2013.

21. Singer, J. W., "Paclitaxel Poliglumex (XYOTAXk, CT-2103): A Macromolecular Taxane", *Journal of Controlled Release*, Vol. 109, pp. 120-126, 2003.

22. Banerjee, S. S., N. Aher, R. Patil, and J. Khandare, "Poly(ethylene glycol)-Prodrug Conjugates: Concept, Design, and Applications", *Journal of Drug Delivery*, Vol. 2012, pp. 1-17, 2012.

23. Liu, S., R. Maheshwari, and K. L. Kiick, "Polymer Based Therapeutics", *Macromolecules*, Vol. 42, No. 1, pp. 3-13, 2009.

24. Satchi-Fainaro, R., M. Puder, J. W. Davies, H. T. Tran, D. A. Sampson, A. K. Greene1, G. Corfas, and J. Folkman, "Targeting Angiogenesis with a Conjugate of HPMA Copolymer and TNP-470", *Nature Medicine*, Vol. 10, No. 3, pp. 255-261, 2004.

25. Gaukroger, K., J. A. Hadfield, L. A. Hepworth, N. J. Lawrence, A. T. Mc Gown, "Novel Synthesis of Cis and Trans Isomers of Combretastatin A-4", *Journal of Organic Chem*istry, Vol. 66, No. 24, pp. 8135-8138, 2001.